POLITECNICO DI MILANO

Scuola di Ingegneria dei Processi Industriali

Corso di Laurea Magistrale in Ingegneria Chimica

Dipartimento di Chimica, Materiali e Ingegneria Chimica "Giulio Natta"

Systematic staging design of fixed-bed methanol synthesis reactor

Relatore: Prof. Flavio Manenti

Tesi di laurea in Ingegneria Chimica di:
Andrés Ricardo León Garzón – Matr. 770771

2012 – 2013

Acknowledgements

To mom, dad and all my family that were with me through this whole experience

To my professor for its support and guidance though all this process

And to my friends with whom I had the most amazing moments these two years in Milan

Contents

Index of figures

Index of tables

Abstract

The present thesis work deals with the techno-economical assessment of the reactor network for methanol synthesis and direct dimethyl ether synthesis from the energy-process integration viewpoint. The reactor network is composed by a water-cooled reactor; a gas-cooled reactor used to preheat the syngas fed to the network; a separation section and a recycle loop. This general configuration is often reduced to the study of the sole water-cooled reactor in literature works. Although such reactor is the key-element of the overall system, the other parts of the process cannot be anymore neglected when the techno-economical assessment is the target of reactor design.

Therefore, the so-called systematic staging design methodology proposed by Hillestad, 2010 [26] is adopted to redefine the optimal ratio between the different stages of methanol synthesis reactor network. To do so, the phenomenological mathematical model of the overall system is required together with the solution of the resulting set of ordinary differential equations coupled with algebraic constraints and initial and boundary conditions as well. It means that beyond the cumbersome issues of mathematical modeling to properly characterize the heterogeneous reactors for methanol and dimethyl ether synthesis, a boundary value problem has to be solved iteratively within an optimization procedure.

According to what has been described, the model is then implemented into a multivariable, nonlinear optimization routine in order to maximize not only the methanol and/or dimethyl ether production but also the steam generation. It is demonstrated that a revision of the traditional design based on the systematic staging design for the integrated optimization of energy and process yield can increase the net operating margin of a medium size methanol synthesis plant by about 2 M€/y.

Estratto

Il presente lavoro di tesi si occupa della valutazione tecno-economica della rete del reattore di sintesi del metanolo e della sintesi diretta dell'etere dimetilico dal punto di vista dell'integrazione processo-energetica. Questa rete è composta da un reattore raffreddato ad acqua bollente; un reattore raffreddato a gas utilizzato per il preriscaldamento del *syngas* alimentato alla rete; una sezione di separazione e un ricircolo. Spesso nella letteratura, la suddetta configurazione viene ridotta allo del studio unicamente del reattore raffreddato ad acqua bollente. Sebbene tale reattore sia l'elemento chiave del sistema, le altre parti del processo non possono essere più trascurate quando la valutazione tecno-economica è l'obiettivo della progettazione del reattore.

Pertanto, la cosiddetta *systematic staging design methodology* proposta da Hillestad, 2010 [26] è stata adottata per ridefinire il rapporto ottimo tra i vari stadi della rete del reattore di sintesi di metanolo. Per fare questo, è necessario il modello matematico e fenomenologico del sistema insieme alla soluzione del set di equazioni differenziali ordinarie accoppiate con i vincoli algebrici e le condizioni iniziale e al contorno. Questo vuol dire che, al di là delle complicazioni nella modellazione matematica per caratterizzare correttamente i reattori eterogenei per la sintesi di metanolo e dell'etere dimetilico, un problema di valori al contorno deve essere risolto in modo iterativo all'interno di una procedura di ottimizzazione.

D'accordo a quanto è già descritto, il modello viene poi implementato in una procedura di ottimizzazione multidimensionale non lineare, allo scopo di massimizzare non unicamente la produzione metanolo e/o etere dimetilico, ma anche la generazione di vapore. È stato dimostrato che un riesame della progettazione tradizionale basato sul *systematic staging design* per l'ottimizzazione integrata di energia e rendimento del processo può aumentare il

margine operativo lordo di un impianto di sintesi di metanolo di media taglia in circa 2 M€ /anno.

Resumen

El presente trabajo aborda la evaluación tecno-económica de la red de reacción para la síntesis del metanol y la síntesis directa del éter dimetílico desde el punto de vista de la integración energética y de procesos. La red de reacción de síntesis está formada por un reactor refrigerado por agua; un reactor refrigerado por gas utilizado para precalentar el gas de síntesis que alimenta la red; una sección de separación y un circuito de recirculación. Frecuentemente en la literatura esta configuración se reduce únicamente al estudio del reactor refrigerado por agua. No obstante, aun cuando este reactor es el elemento clave del sistema, los otros segmentos del proceso no pueden ser excluidos cuando la evaluación tecno-económica es el objetivo del diseño de reactores.

Por lo tanto, la llamada *systematic staging design methodology* propuesta por Hillestad, 2010 [26] fue adoptada para redefinir la relación óptima entre ambas etapas (reactor refrigerado con agua y a gas) de la red de reacción de síntesis de metanol. Para ello, el modelo matemático y fenomenológico del sistema es necesario junto con la solución del conjunto resultante de ecuaciones diferenciales ordinarias con sus respectivas restricciones algebraicas y sus condiciones iniciales y al contorno. Esto significa que, más allá de la intrincada proposición del modelo matemático para caracterizar adecuadamente un reactor heterogéneo para la síntesis de metanol y éter dimetílico, un problema de valor al contorno tiene que resolverse de forma iterativa dentro de un procedimiento de optimización.

De acuerdo a lo descrito anteriormente, el modelo es empleado posteriormente en una rutina de optimización multiobjetivo no lineal con el fin maximizar no sólo la producción de metanol y/o éter dimetílico, sino también la generación de vapor. Está demostrado que una revisión del diseño tradicional basada en el procedimiento de *systematic staging design* para la optimización integral del rendimiento energético y de proceso puede aumentar el

margen de beneficio de una planta de síntesis de metanol de tamaño medio en cerca de 2 M€/año.

1. Introduction

With a chemical composition of CH_3OH, methanol (MeOH) is the simplest of the alcohols and an important chemical used as a building block in a variety of industries including chemical, petrochemical, polymer and pharmaceutical industries. It is also an energy carrier since is an excellent fuel for transportation mediums based on internal combustion engines; is a precursor in the production of biodiesel through the transesterification of vegetable oils and animal fats; is employed in the Methanol to Gasoline (MTG) to produce gasoline; and is a suitable combustible for direct methanol fuel cells (DMFCs) as it able to react with air to produce electric energy [41]; a distribution of methanol utilization can be seen on Figure 1-1. Nowadays, as crude oil prices keep raising and its global production seems to have arrived to its ceiling [39], exploration and development of alternative fuels has become essential and interest in methanol is growing up not only at the industrial level but also at an academic level up to a point where a new "Methanol Economy" (see Figure 1-2) has been proposed as an alternative to the hydrogen economy thanks to its evident benefits as explained before.

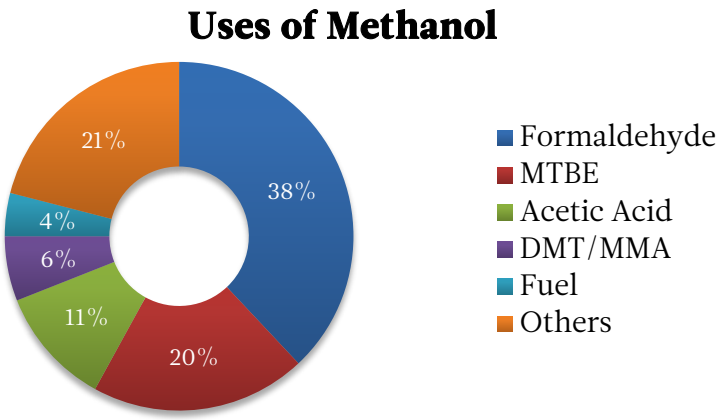

Figure 1-1 Principal uses of methanol [41].

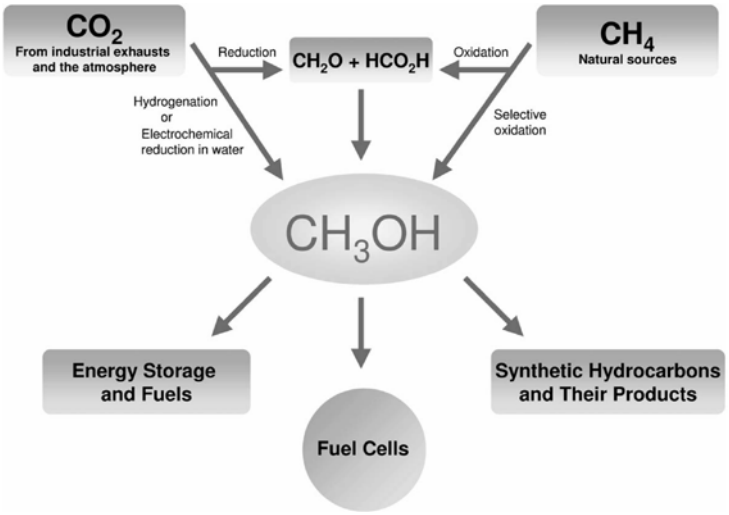

Figure 1–2 The "Methanol Economy" [41].

Methanol is currently produced from natural gas through the catalytic reaction of syngas; the four main parts that constitutes the methanol synthesis process from syngas are: feed purification, steam reforming of syngas, methanol synthesis and methanol purification. Furthermore, it is suggested that methanol could be produced from the chemical recycling of CO_2 derived from the industrial combustion of fossil fuels and possibly the CO_2 present on the atmosphere [41] as seen on Figure 1–3.

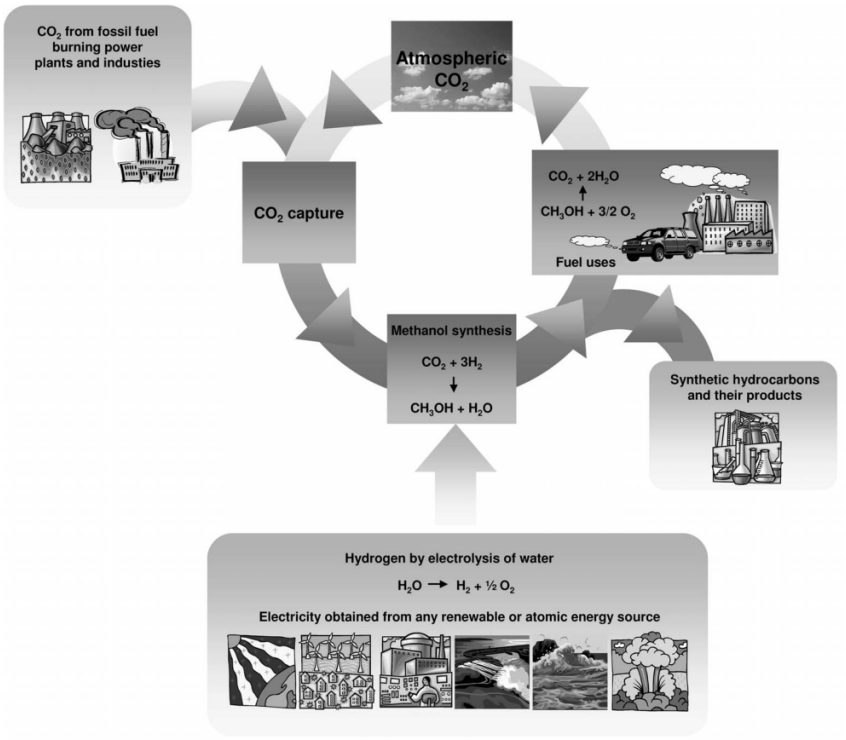

Figure 1–3 MeOH and hydrocarbons production throughout the recycle of CO_2 [41].

Historically, methanol was first produced by destructive distillation of wood and it was not until the 1920s that the first catalytic synthesis process from syngas was developed by the Badische Anilin- & Soda-Fabrik (BASF); this process used a ZnO/Cr_2O_3 catalys and operated at temperatures from 350 to 450˚C and at pressures ranging from 250 to 350 atm, thus acquiring the name of *high-pressure methanol synthesis*, by the time, syngas was mainly produced by coal or coke gasification resulting in a gas with high sulfur content, although the catalyst was highly stable to impurities [31]. Through the 1960s another process was developed as a result of a shift on the production of syngas from coal to natural gas, this resulted in a syngas with lower levels of impurities and allowed to use more active catalysts and less severe operating conditions [41]. As a result, the Imperial Chemical Industries (ICI) developed a new process using a $CuO/ZnO/Al_2O_3$ catalyst. Such process operates at temperatures ranging from 200 to 300˚C and pressures from 50 to 100 atm, hence obtaining the name of *low-pressure methanol synthesis* [31]. Several variants of the low-pressure methanol synthesis technology have been proposed, however they are mostly based on the ICI catalyst and differ essentially on the reactor design and the catalyst configuration.

On the other hand, dimethyl ether (DME) is the simplest of the ethers with a composition of CH_3OCH_3, DME is employed mainly as a household fuel when it's blended with liquefied petroleum gas (LPG) for domestic cooking and heating [27] or is used as an aerosol propellant for spray cans replacing the hazardous CFCs [41]. Nevertheless, numerous investigations have been carried out in order to determine its suitability as a fuel in compression ignition with direct injection engines. As a result, DME is a promising efficient alternative fuel for diesel engines as it possesses a high cetane number, produces a smoke-free combustion due to its high oxygen content and has a low boiling point that allows a quick vaporization inside the engine cylinders [3].

Dimethyl ether is produced almost entirely by the catalyzed (usually gamma-Al_2O_3 or H-ZSM-5) dehydration of methanol in either a two-step or a one-step process; the two-step process is characterized by a first reactor in which methanol is produced from syngas to later being dehydrated in a second reactor to produce DME; the one-step process combines both reactions on a single reactor using a dual catalytic system.

The present work is motivated as a preliminary approach to a future problematic in which alternative clean fuels are required not only to look for a replacement of the depleting fossil fuels but also to address all the issues regarding environmental aspects that are a concern

for present society. As a result, Gas-to-Liquids (GTL) technology is presented as a commercially-viable way to address such issues [56]; this technologies is aimed towards the monetization of natural gas into liquids such as MeOH and DME, nonetheless an active topic in research nowadays comprise the utilization of non-traditional feedstock like biomass or biogas can in order to create a carbon neutral cycle for the production of fuels (e.g. see Figure 1-4).

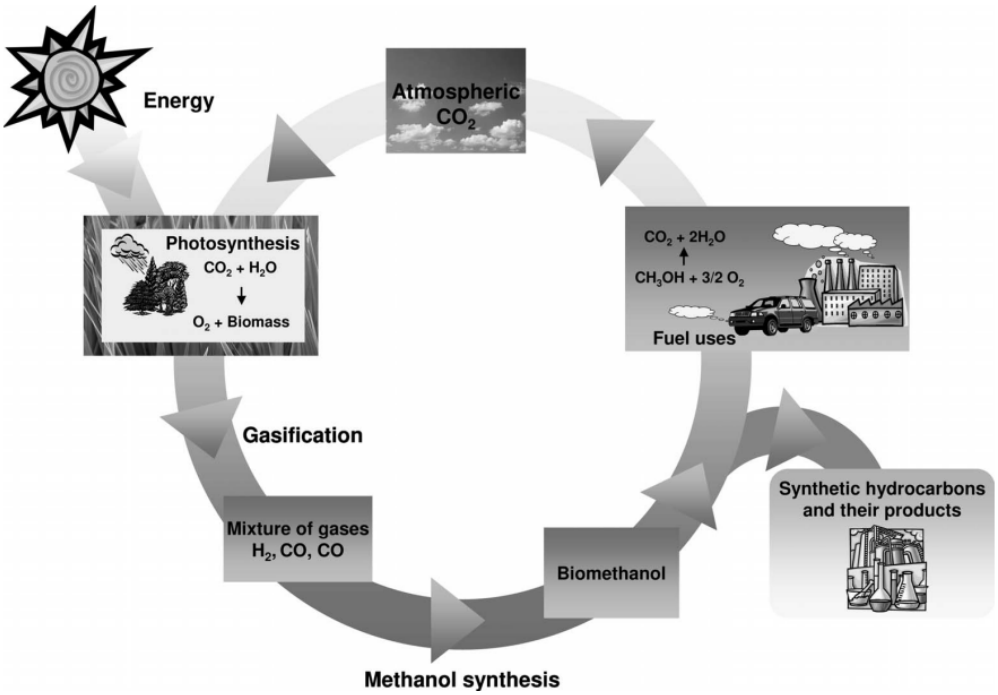

Figure 1-4 Methanol production through a neutral carbon cycle [41].

Considering the previous reasons and founded in the approach proposed by Hillestad, 2010 [26], this thesis activity is aimed towards the application of the systematic staging to the optimal design of the methanol synthesis network and eventually of the direct dimethyl ether synthesis network. Such network consists basically of a well-established technology of fixed-bed reactors in the Lurgi type process [34] together with a separation and recycle system. In the direct dimethyl ether synthesis network, the methanol production is coupled with the DME production in the one-step process that takes advantage of the equilibrium-unlimited dehydration of methanol overcoming the limitations imposed by the equilibrium thermodynamics of methanol synthesis reaction [31].

Raw materials from a traditional feedstock was used throughout the calculations, however the approach described above allows to obtain a high degree of flexibility in the modeling, and therefore, using raw materials from non-traditional feedstocks impose no problem to the model and ensures a future proof solution that is in line with present research subjects.

2. Methanol Synthesis: General Description

2.1 State of the art

Several technologies have been developed since the introduction of the ICI *low-pressure methanol synthesis* as it is the basis of the current processes of methanol production. Therefore, these technologies use the same Cu-based catalyst and differ from each other basically on the catalyst composition and the reactor configuration.

Among the current technologies, a shell and tube reactor is used by Lurgi GmbH, Haldor Topsøe A/S and Davy Process Technology Ltd. Lurgi GmbH employs a dual stage reactor first a water-cooled reactor followed by a gas-cooled reactor, the first reactor uses boiling water to control the temperature while the second reactor uses fresh inlet syngas as cooling medium, thus, a smaller preheater is used; Haldor Topsøe A/S employs a single boiling water reactor; and finally Davy Process Technology Ltd uses either a gas-cooled reactor, a boiling water reactor or a radial flow boiling water reactor [13,25,34].

Other technologies include Casale Group that uses a pseudo isothermal reactor consisting of cooling plates submerged in the catalyst bed, inside the plates a cooling fluid flows, these include fresh inlet syngas, water or other heat transfer fluid; and Air Products and Chemicals, Inc. uses a liquid phase methanol (LPMeOH) process in a slurry reactor, inside the reactor, fine catalyst particles are entrained in an inert hydrocarbon liquid that works as a heat sink [10,52].

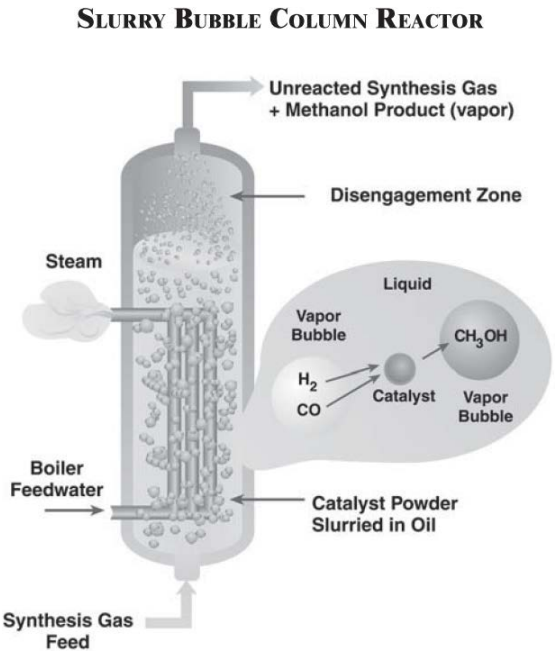

Figure 2-1 LPMeOH process slurry bubble reactor [52]

As already stated each technology uses an ICI-based catalyst that differ from each other basically on its constituent's composition, it is also important to mention that each technology includes solutions for the upstream and downstream operations the methanol synthesis reactor.

The gas exiting the reactor is cooled to condensate the crude methanol and it is later separated from the gas in a vertical drum, the gas fraction is recycled back to the reactor and a fraction is purged to avoid the buildup of inert components within the system while the crude methanol is directed to the distillation section.

Crude methanol is composed of methanol, water and other impurities, such impurities can be light or heavy ends and their nature and amount depend on the feed, reactor conditions and the type of catalyst. Light ends include dissolved gases and other hydrocarbons as methyl formate, acetone and dimethyl ether while the heavy ends include a variety of components like higher alcohols, ketones, esters and long chain hydrocarbons [18].

Impurities are separated typically in two stages, in the first stage all the components with a lower boiling point than methanol are removed in the light ends column. Subsequently, a second column perform the separation of methanol, obtained at the top from a side-stream below the pasteurization section; from the heavy ends, obtained as a side-stream; and the water, obtained at the bottom of the column [11].

2.2 Physicochemical aspects of methanol synthesis

As previously specified, methanol is mainly obtained from methane through the catalytic reaction of syngas. As a result, the three principal reactions involved are: hydrogenation of carbon monoxide (2.1), the water gas shift reaction (WGS) (2.2) and the hydrogenation of carbon dioxide (2.3).

$$CO + 2H_2 \leftrightarrow CH_3OH \qquad \Delta H_{298K} = -90.55\ kJ/mol \qquad 2.1$$

$$CO_2 + H_2 \leftrightarrow CO + H_2O \qquad \Delta H_{298K} = +41.12\ kJ/mol \qquad 2.2$$

$$CO_2 + 3H_2 \leftrightarrow CH_3OH + H_2O \qquad \Delta H_{298K} = -49.43\ kJ/mol \qquad 2.3$$

As can be observed from the precedent equations, the three reactions are not independent from each other as one is a linear combination from the other two.

Several byproducts can also be formed due to the presence of traces of contaminants in the catalyst as can be seen on Table 2-1; the formation of such byproducts can be limited modifying not only the catalyst constituents or the feed gas composition but also the temperature and the residence time within the reactor [18].

Table 2-1 Byproducts present on the methanol synthesis process.

Higher alcohols formed by traces of alkali	$nCO + 2nH_2 \leftrightarrow C_nH_{2n+1}OH + (n-1)H_2O$
Hydrocarbons and waxes formed by traces of iron, cobalt and nickel	$CO + 3H_2 \leftrightarrow CH_4 + H_2O$ $CO_2 + 4H_2 \leftrightarrow CH_4 + 2H_2O$ $nCO + (2n-1)H_2 \leftrightarrow C_nH_{2n+2} + nH_2O$
Esters	$(CH_2O)_{ads} + (RCHO)_{ads} \leftrightarrow CH_3COOR$
Dimethyl ether	$2CO + 4H_2 \leftrightarrow CH_3OCH_3 + H_2O$
Ketones	$RCH_2CH_2OH \leftrightarrow RCH_2CHO + H_2$ $2RCH_2CHO \leftrightarrow RCH_2COCHRCH_3 + O_{ads}$

Limiting the extent of byproducts formation through the feed gas composition is done modifying the stoichiometric number S (2.4).

$$S = \frac{moles\ H_2 - moles\ CO_2}{moles\ CO + moles\ CO_2} \qquad 2.4$$

Values below 2 indicate a deficit of hydrogen in the syngas while greater values indicate an excess of hydrogen. Ideal values for the stoichiometric number are 2 or slightly above it, in this way it's possible to control the formation of byproducts. To exemplify, syngas produced from coal gasification has less than the optimum value of hydrogen content, whereas syngas coming from steam reforming of methane have values around 2.8 to 3.0 [41]. Nevertheless, a value of stoichiometric factor equal to 4 is selected in the present work as it is not only compatible with the industrial interest but also allows an improved controllability of the process [12].

2.2.1 Thermodynamics & kinetics

The production rate of methanol is affected typically by thermodynamic equilibrium limitations. An initial analysis can be made from equations 2.1, 2.2 and 2.3 from which it's possible to appreciate that the overall system is exothermic and as a consequence low temperature favors the overall conversion, nonetheless reducing the temperature penalizes the kinetics of reaction. A plot of $\log(K)$ $vs. T$ illustrates the dependence of the equilibrium constant with the temperature in Figure 2-2.

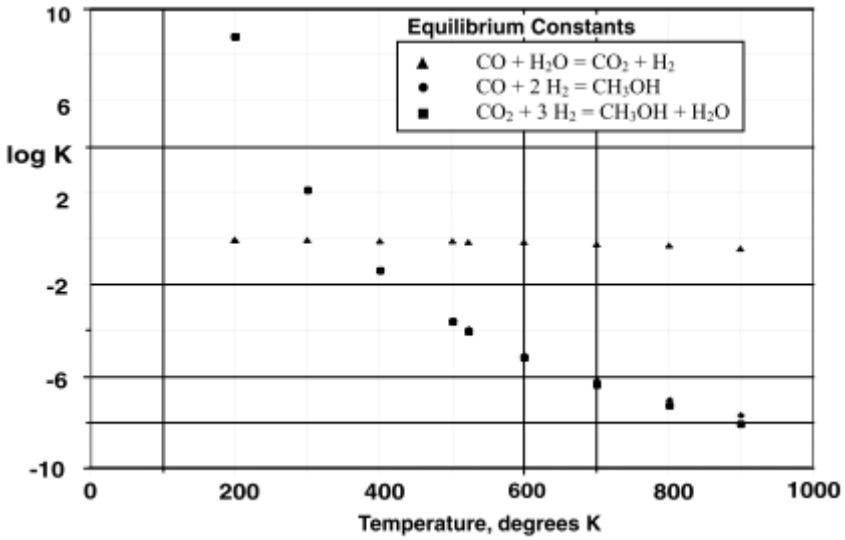

Figure 2-2 Dependence of the equilibrium constant with temperature [31].

As a result, the synthesis process is carried out at high temperatures which comprise a series of complications mostly linked to the exothermicity of the reaction making the thermal control of critical importance to avoid the deactivation of the catalyst by sintering.

Additionally, it can be observed from Figure 2-2, the WGS equilibrium constant is not sensitive to the temperature; therefore such reaction is still significant in a wide range of temperatures. Another important aspect is its low equilibrium constant that allows reversing the reaction equilibrium by modifying the partial pressures of the species. Both aspects results on a high impact on the final product composition of the WGS reaction [31].

A further analysis can be made in terms of pressure, reactions 2.1 and 2.3 are characterized by a decrease on the number of moles and consequently a high pressure favors likewise the conversion to methanol. However, a higher pressure involves higher capital investment, higher energy demands and further operational complications.

The kinetic model used in this work is the one proposed by Graaf, Stamhuis & Beenackers in 1988 [22], the reaction rates are illustrated on equations 2.5, 2.6 and 2.7 and are based on the commercial $CuO/ZnO/Al_2O_3$ catalyst.

$$r_1 = \frac{k_1 K_{CO}\left[f_{CO} f_{H_2}^{1.5} - \frac{f_{CH_3OH}}{f_{H_2}^{0.5} K_{P1}}\right]}{\left(1 + K_{CO} f_{CO} + K_{CO_2} f_{CO_2}\right)\left[f_{H_2}^{0.5} + \left(\frac{K_{H_2O}}{K_{H_2}^{0.5}}\right) f_{H_2O}\right]} \qquad 2.5$$

$$r_2 = \frac{k_2 K_{CO_2}\left[f_{CO_2} f_{H_2} - \frac{f_{CO} f_{H_2O}}{K_{P2}}\right]}{\left(1 + K_{CO} f_{CO} + K_{CO_2} f_{CO_2}\right)\left[f_{H_2}^{0.5} + \left(\frac{K_{H_2O}}{K_{H_2}^{0.5}}\right) f_{H_2O}\right]} \qquad 2.6$$

$$r_3 = \frac{k_3 K_{CO_2}\left[f_{CO_2} f_{H_2}^{1.5} - \frac{f_{CH_3OH} f_{H_2O}}{f_{H_2}^{1.5} K_{P3}}\right]}{\left(1 + K_{CO} f_{CO} + K_{CO_2} f_{CO_2}\right)\left[f_{H_2}^{0.5} + \left(\frac{K_{H_2O}}{K_{H_2}^{0.5}}\right) f_{H_2O}\right]} \qquad 2.7$$

Where $r_1$is for CO hydrogenation, r_2 is for the WGS reaction and r_3 is for the CO_2 hydrogenation. The kinetic parameters were determined as a function of temperature from 483 K to 518 K and explained with a dual site Langmuir-Hinshelwood mechanism based on dissociative hydrogen adsorption. CO and CO_2 adsorb competitively on the site 1, while H_2 and H_2O adsorb competitively on the site 2; for the three parallel reactions a rate determining step (RDS) was determined through a χ^2 test and consequently the rate of reaction was taken as that of the RDS [22]. Nonetheless, the mechanism is still under discussion in the scientific community.

The kinetic parameters, adsorption equilibrium constants and chemical equilibrium constants are provided in the Appendix A.

2.3 Catalyst

As already stated, commercial catalysts used for the low pressure methanol synthesis are made of a mixture of copper oxide and zinc oxide stabilized with alumina, the activity of this catalyst is higher than the previous high pressure synthesis catalyst, therefore allows operating at low temperatures (200 to 300˚C) and evidently at low pressures (50 to 100 atm).

Numerous industrial methanol synthesis processes employ this catalyst, only differing on the composition of the mixture. The catalyst is prepared by a coprecipitation method in which nanoparticles of CuO and ZnO are precipitated on the porous support of Al_2O_3 which acts as a structural promoter, the CuO particles are alternatively arranged as the ZnO has the function of a spacer, something that assist to generate the large surface areas of these catalysts (20 – 30 m^2/g) [5,18,41].

Copper catalysts are highly selective and the production of by-products associated to the high pressure synthesis were significantly reduced or eliminated, nevertheless they are greatly sensitive to poisons such as sulfur or halogenated compounds. Therefore, the synthesis gas employed for the methanol synthesis must be extremely pure. Deactivation by sintering is also important on copper catalyst and fusing as copper clusters begin to migrate and merge at temperatures above 227˚C reducing the surface area while beyond temperatures of 280 – 300˚C the catalyst will suffer permanent damage. As a result, a proper temperature control must be guaranteed along the reactor to avoid its deactivation. Usually, copper catalysts have a life cycle of about 2 to 5 years [18,31,50].

3. Dimethyl Ether Synthesis: General Description

3.1 State of the art

Conventionally, dimethyl ether has found application as an aerosol propellant replacing the harmful chlorofluorocarbons (CFC), nonetheless; as it is non-toxic, environmentally friendly, biodegradable and has properties similar to LPG; new markets for DME are being explored for its use as LPG blend stock, transportation fuel, fuel for power generation turbines and as chemical intermediate to olefins and gasoline production (Methanol to olefins (MTO) or methanol to gasoline (MTG) as seen on Figure 3-1). As a result, DME is the fastest-growing methanol derivative even when it's still an emerging business [19].

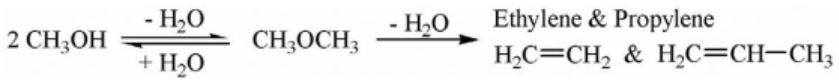

a)

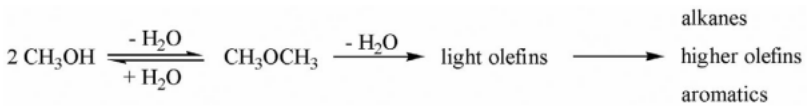

b)

Figure 3-1 a) Methanol to olefin (MTO) pathway and b) Methanol to gasoline pathway (MTG) [41].

Traditionally, dimethyl ether has been produced in a two-step process or also called indirect process, it is characterized by the utilization of a single reactor to produce methanol through the technologies already discussed in the previous chapters and a second reactor used to the catalytic dehydration of methanol in order to produce dimethyl ether [15].

On the other hand, research on novel technologies and methods is still ongoing for the synthesis of dimethyl ether in a one-step process or direct process that employs a

bifunctional catalyst or catalyst mixture, such catalyst must have a hydrogenating characteristic to produce methanol, that act as an intermediate, and a dehydration property that is responsible for the synthesis of DME. The direct process occurs normally at temperatures ranging from 210˚C to 290˚C and with pressures around 3 to 10 MPa [15] and the synthesis technologies include the utilization of a fixed-bed or fluidized bed reactor [30].

Another novel process is based on the same technology of the liquid phase methanol (LPMeOH) process, therefore implies the utilization of the utilization of the bifunctional catalyst in a slurry reactor. The technology, called liquid phase dimethyl ether (LPDME) process, achieves twice a conversion of CO in comparison to LPMeOH [55], nonetheless the mass transfer resistances induced by the presence of the liquid phase reduces the yield and conversion in comparison with the gas phase fixed bed process [30].

The operations downstream the reactor are conceived to separate the products and to the recycle of the unreacted syngas. In this thesis work, the flash drum separator usually adopted to roughly separate light ends (CO, CO_2, H_2, CH_4, and N_2) from a liquid mixture of dimethyl ether is simulated, whereas the modeling and optimization of the downstream system to purify the products is out of the scope of this thesis and it is considered an important future development, methanol and water. This liquid fraction is sent to a stripper where the dissolvedCO_2 is separated and then, the DME is separated from water and methanol by distillation, DME purity depends on its final application. At last, water and methanol are separated in an ad-hoc distillation unit.

3.2 Physicochemical aspects of direct dimethyl ether synthesis

Direct dimethyl ether synthesis couples the reactions involved in the hydrogenation of syngas with that for the dehydration of methanol throughout the use of a bifunctional catalyst or a catalyst mixture, the reactions involved are:

Hydrogenation of CO:

$$CO + 2H_2 \leftrightarrow CH_3OH \qquad \Delta H_{298K} = -90.55\ kJ/mol \qquad 3.1$$

Hydrogenation of CO_2:

$$CO_2 + 3H_2 \leftrightarrow CH_3OH + H_2O \qquad \Delta H_{298K} = -49.43\ kJ/mol \qquad 3.2$$

Water gas shift (WGS):

$$CO_2 + H_2 \leftrightarrow CO + H_2O \qquad \Delta H_{298K} = +41.12\ kJ/mol \qquad 3.3$$

Dehydration of methanol:

$$2CH_3OH \leftrightarrow CH_3OCH_3 + H_2O \qquad \Delta H_{298K} = -23.4\ kJ/mol \qquad 3.4$$

Coupling reactions 3.1 with 3.4 and 3.2 with 3.4 the following reactions are obtained:

Direct synthesis of DME from CO hydrogenation:

$$2CO + 4H_2 \leftrightarrow CH_3OCH_3 + H_2O \qquad \Delta H_{298K} = -204.5\ kJ/mol \qquad 3.5$$

Direct synthesis of DME from CO_2 hydrogenation:

$$2CO_2 + 6H_2 \leftrightarrow CH_3OCH_3 + 3H_2O \qquad \Delta H_{298K} = -122.26\ kJ/mol \qquad 3.6$$

According to Jia, Tan & Han, 2006 [28], the CO hydrogenation is more advantageous than CO2 hydrogenation as the equilibrium concentration of DME is higher for the first case. This is explained by the fact that methanol (intermediate in the production of DME) productivity in CO2 hydrogenation is low as such reactions is competing with the WGS reaction that is generally faster, on the other hand as the WGS reaction is proceeding forwards, producing CO and H2O, the production of the latter is detrimental to the equilibrium conversion of the CO2 hydrogenation to methanol and consequently to dimethyl ether.

Nonetheless, the presence of CO_2 is beneficial as it has a high heat capacity that can regulate temperature, in the other hand the presence a small quantity of CO_2 in the syngas mixture is beneficial as it helps preventing the deposition of coke over the copper catalyst that could result in its deactivation [41] and increases the selectivity towards DME [54]. On the other hand, according to Moradi, Ahmadpour, Yaripour & Wang, 2011 [38] increasing the H_2/CO ratio results in a higher conversion of CO and a higher DME selectivity and yield while also decreases the CO_2 selectivity produced by the WGS reaction.

3.2.1 Thermodynamics & kinetics

Similar to the methanol synthesis reaction, the dehydration of methanol is affected by thermodynamic equilibrium; nonetheless such limitation is not as detrimental and the combination of these reactions will cause a synergistic effect alleviating the methanol synthesis equilibrium limitation as it is consumed to produce dimethyl ether according to reaction 3.4 depressing the effect of the reverse reactions 3.1 and 3.2. This is translated in a higher once through syngas conversion.

The effect of temperature for the methanol synthesis reaction was explained in section 2.2.1, dimethyl ether synthesis reaction is affected the same way as it is an exothermic reaction and therefore increasing the temperature is detrimental to the equilibrium conversion of the reacting species. Higher temperature has also an adverse effect on the catalyst activity as it causes the sintering of copper. On the other hand, dimethyl ether synthesis reaction does not lead to a change in the number of moles and is not affected by a change on the system pressure; however thanks to the synergetic effect a higher pressure favors the overall syngas conversion as the methanol synthesis is a mole decreasing reaction, however, according to Ereña, Garoña, Arandes, Aguayo & Bilbao, 2005 [16] the reaction parameters are barely affected for pressures above 50 bar.

The most common kinetic model for the direct synthesis of dimethyl ether is coupling two kinetic models one for the methanol synthesis from syngas (CO hydrogenation and CO_2 hydrogenation) and one for the methanol dehydration. On section 2.2.1 the Graaf model was introduced for the methanol synthesis reactions; such model was coupled with the Berčič & Levec, 1992 [6] model for the dehydration of methanol over γ-Al_2O_3 catalyst:

$$r_4 = \frac{k_4 K_{CH_3OH}^2 \left(C_{CH_3OH}^2 - \frac{C_{H_2O} C_{DME}}{K_{C4}} \right)}{\left(1 + 2\left(K_{CH_3OH} C_{CH_3OH} \right)^{1/2} + K_{H_2O} C_{H_2O} \right)^4} \qquad 3.7$$

Where C_i is the concentration of the $i\text{-}th$ species. The rate equation was obtained assuming a Langmuir-Hinshelwood mechanism where the RDS is the surface reaction and that a dissociative adsorption of methanol is taking place on the surface of the catalyst. In the denominator of equation 3.7 the adsorption term for DME is neglected as its adsorption constant was too small in comparison with the other terms.

The kinetic parameters for the methanol dehydration reaction are listed in the Appendix B.

3.3 Catalyst

As explained before, a bifunctional catalyst is composed by a metallic function that allows the hydrogenation of CO and CO_2 to produce methanol and an acid function that assures the production of dimethyl ether by the dehydration of methanol. Typically, the metallic function is composed by the well-established $CuO/ZnO/Al_2O_3$ while the acid function is

normally composed by γ-Al_2O_3, the bifunctional catalyst is normally prepared by a co-precipitation/sedimentation method with a mass ratio of 2:1 [17,29].

Similar to the methanol catalyst, the bifunctional catalyst suffers from deactivation by the presence of impurities or by thermal sintering, nonetheless such catalyst suffers additional deactivation by coke deposition that is presumably produced by the degradation of methoxy groups, as coke is deposited it blocks initially the metallic functions then expanding to the Al_2O_3 support to finally block the acid function of the catalyst [46]. Another drawback of the γ-Al_2O_3 catalyst is the tendency to absorb water more strongly than methanol due to its higher polarity, and therefore it could block active sites of the catalyst deactivating it [2].

4. Methanol & DME Synthesis: Mathematical Model

4.1 Methanol synthesis

4.1.1 Pseudo-homogenous model

The present work is based on an already consolidated technology as it is the Lurgi type reactor [34]. As illustrated on Figure 4-1, syngas is fed to the shell side of the gas-cooled (GaC) reactor where it is pre-heated by the hotter process stream flowing within the tubes. The pre-heated syngas is then fed to the tube side of the water-cooled reactor (WaC), where the catalyst for methanol synthesis is present. The syngas fed to the fixed-bed of the catalytic tube bundle is partially converted into methanol along the first reactor. The methanol synthesis is particularly exothermic and the shell side is filled of boiling water to preserve the desired operating conditions of the WaC reactor. The intrinsic intensified nature of modern methanol process allows combining the methanol conversion to the medium pressure steam generation. The outflow of the WaC reactor is fed to the tube side of the GaC reactor where the methanol synthesis continues. GaC temperature profile is controlled exchanging with the fresh inlet syngas to be pre-heated in countercurrent in the shell side. The GaC reactor outflow is then sent to a downstream separation process where the methanol is recovered and the unreacted syngas is recycled back unless a purge system to remove by-products, and accumulations of incondensable gas.

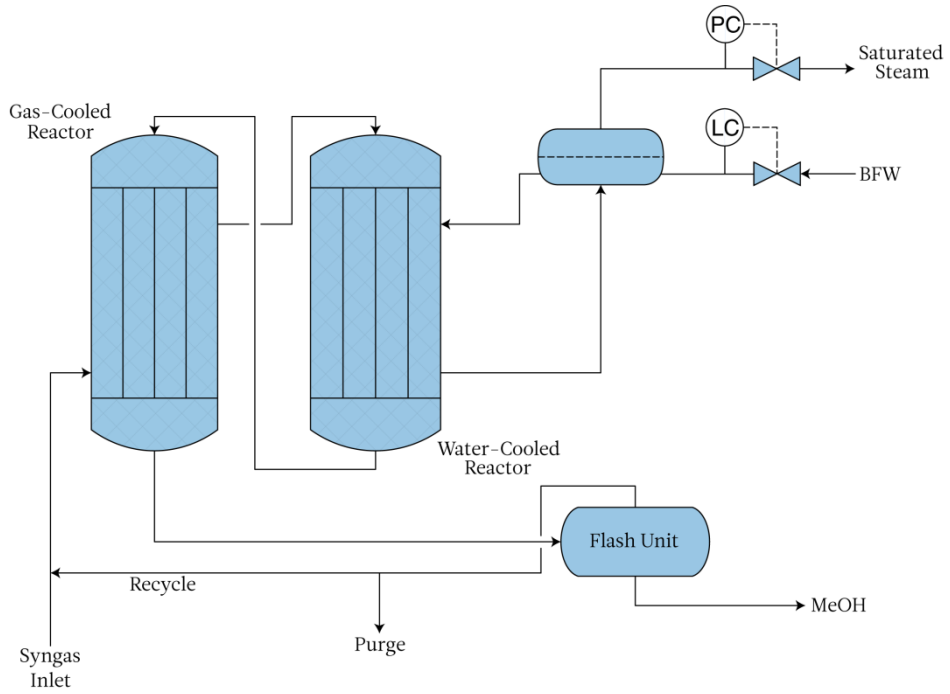

Figure 4-1 Methanol synthesis loop.

A pseudo homogeneous model was used for both the WaC and the GaC reactors; it is based on the work by Manenti, Cieri & Restelli, 2011 [35], in such model the following assumptions were made for the simulation of the plug flow reactor (PFR):

a) Negligible axial diffusion: dispersion of the species through the reactor is not considered.
b) Negligible radial diffusion: concentration and temperature along the radial direction is constant.
c) Constant radial velocity.
d) Homogeneous catalytic particle: no temperature or concentration gradients inside the particle.
e) Negligible catalyst deactivation.
f) Negligible side reactions due to the high selectivity of the catalyst.

The previous assumptions are reasonable for the steady state simulation and its results are in good agreement with those of a more rigorous heterogeneous model as stated by Manenti et al., 2011 [35].

The efficiency of the catalytic particle is obtained through a modified Thiele modulus (Equations 4.1 and 4.2) based on the mathematical modeling of the internal mass transfer limitations work of Lommerts, Graaf & Beenackers , 2000 [32]. It is a simplification of more

complicated models such as the dusty-gas or the Stefan Maxwell equations; however, the modified Thiele modulus provides reasonable results and its application is not computationally demanding.

$$\phi_i = \frac{r_P}{3}\sqrt{\frac{k'_j\left(k_j^{eq}+1\right)}{\mathcal{D}_{i,eff}^{j}k_j^{eq}}} \qquad 4.1$$

$$\eta_i = \frac{1}{\phi_i}\frac{(3\phi_i\, coth(3\phi_i)-1)}{3\phi_i} \qquad i = 1,2,3 \qquad 4.2$$

In the previous equations ϕ_i is the modified Thiele modulus, r_P is the radius of the catalytic pellet, k'_j is the pseudo-first-order constant of the j-th reaction, k_j^{eq} is the equilibrium constant of the j-th reaction; $\mathcal{D}_{i,eff}^{j}$ is the effective diffusivity of the j-th component of the mixture. The values of k'_j are obtained through a linearized kinetics (Equations 4.3 and 4.4) for methanol and water as described by Lommerts et al., 2000 [32].

$$r'_{CH_3OH} = k'_j\left(C_{H_2} - \frac{C_{CH_3OH}}{k_{CH_3OH}^{eq}}\right) \qquad 4.3$$

$$r'_{H_2O} = k'_j\left(C_{H_2} - \frac{C_{H_2O}}{k_{H_2O}^{eq}}\right) \qquad 4.4$$

The proposed balance equations for the tube side of both the WaC and the GaC reactor are shown on equations 4.5, 4.6 and 4.7. Moreover, an energy balance for the shell side of the GaC reactor shown on equation 4.8 is coupled to the aforementioned balances.

WaC and GaC mass balance:

$$\frac{M}{A_{int}}\frac{d\omega_i}{dz} = MW_i\rho_{cat}(1-\varepsilon_b)\sum_{j}^{NR}\nu_{ij}\eta_j r_j \qquad 4.5$$

WaC and GaC energy balance:

$$\frac{Mc_{p_{mix}}}{A_{int}}\frac{dT}{dz} = \pi\frac{d_{int}}{A_{int}}U_{tube}(T_{shell}-T) + \rho_{cat}(1-\varepsilon_b)\sum_{j}^{NR}\left(-\Delta H_j^{rxn}\right)\eta_j r_j \qquad 4.6$$

Ergun equation:

$$\frac{dP}{dz} = -\left(1.75 + 150\left(\frac{1-\varepsilon_b}{Re}\right)\right)\frac{u^2\rho_{gas}}{d_p}\left(\frac{1-\varepsilon_b}{\varepsilon_b^3}\right) \qquad 4.7$$

GaC's shell energy balance:

$$\frac{Mc_{p_{mix}}}{A_{int}}\frac{dT_{shell}}{dz} = -\pi\frac{d_{int}}{A_{int}}U_{shell}(T - T_{shell}) \quad 4.8$$

The minus sign on equation 4.8 takes account of the fact that the syngas flows in countercurrent direction in the shell side.

It is worth noting that the mass balance on equation 4.5 is formulated in mass fractions, this allows circumventing a series of complications such as:

a) Avoiding significant deviations due to the assumption of constant moles inside the reactor, as a result, the final methanol fraction is generally underestimated and the remaining fractions are biased as well.
b) The application of global molar balances that account for the decrease on the number of total moles, a characteristic inherently of the methanol synthesis process from syngas.
c) The use of methods that continuously update the molar fractions of the species along the reactor that can lead to numerical instabilities in the solution of the model.

As already indicated, downstream the reactor is present a separation unit that consist of a flash vessel, in this unit the gases, comprising the light ends CO, CO_2, H_2, N_2 and CH_4, are separated from a liquid phase that contains a mixture of methanol and water. The mass balances of such unit are:

Total mass balance:

$$F = V + L \quad 4.9$$

Component mass balance:

$$Fz_i = Vy_i + Lx_i \quad 4.10$$

$$\sum_{i=1}^{N} y_i = 1 \quad 4.11$$

$$\sum_{i=1}^{N} x_i = 1 \quad 4.12$$

Given flash separator conditions, the solution is found adopting the method proposed by Rachford & Rice, 1952 [43]:

$$f(V/F) = \sum_{i=1}^{N} \frac{z_i(K_i - 1)}{\frac{V}{F}(K_i - 1) + 1} = 0 \qquad 4.13$$

Where K_i are the K-values of an appropriate equation of state:

$$K_i = \frac{y_i}{x_i} = \frac{\phi_i^L}{\phi_i^V} \qquad 4.14$$

The gas outflowing the flash unit is purged in order to avoid accumulation of inerts and then is recycled back to the reactor; the liquid phase is leaded to a successive purification unit that is outside the scope of the present work. All the different correlations used to estimate the physical properties of pure substances and the properties of the mixture as well are available within the Appendix A.

4.1.2 Operational conditions

Operational conditions of the methanol synthesis reactor are described on Table 4-1.

Table 4-1 Operating conditions for methanol synthesis

Feed's molar fractions	CO	0.046
	CO_2	0.094
	H_2	0.659
	H_2O	0.0004
	CH_3OH	0.005
	N_2	0.093
	CH_4	0.1026
Feed molar flow	0.64	mol/tube/s
Pressure	7.698	MPa
Flash temperature	313.0	K
Flash pressure	7.5	MPa

Operational conditions were based on the work reported by Manenti et al., 2011 [35] and Rahimpour, 2008 [44].

4.2 Direct dimethyl ether synthesis

4.2.1 Pseudo-homogeneous model

The model for the synthesis of dimethyl ether employs the same pseudo-homogeneous model described in section 4.1.1, the only modification introduced were the incorporation of an additional mass balance corresponding to the dimethyl ether species; the modification of the existing methanol and water mass balance as well as the heat balance to take account of the methanol's dehydration reaction and the addition of a particle mass balance to take account of the diffusivity resistance through the effectiveness factor for the dimethyl ether reaction.

The particle mass balance is based on the work developed by Song, Cho, Lee, Park & Yoon, 2008 [48], it is worth noting that the temperature gradient is assumed negligible so the energy balance is not considered, the mass balances are represented in equations 4.15, 4.16 and 4.17.

$$\frac{d^2C_{H_2O}}{dr^2}+\frac{2}{r}\frac{dC_{H_2O}}{dr}=-\frac{\rho_P}{2\cdot D_{eff,H_2O}}r_4 \qquad 4.15$$

$$\frac{d^2C_{DME}}{dr^2}+\frac{2}{r}\frac{dC_{DME}}{dr}=-\frac{\rho_P}{2\cdot D_{eff,DME}}r_4 \qquad 4.16$$

$$\frac{d^2C_{MeOH}}{dr^2}+\frac{2}{r}\frac{dC_{MeOH}}{dr}=\frac{\rho_P}{D_{eff,DME}}r_4 \qquad 4.17$$

With the following boundary conditions:

$$\begin{aligned} r=R \quad & C_i=C_{i,bulk} \\ r=0 \quad & \frac{dC_i}{dr}=0 \end{aligned} \qquad 4.18$$

Where r is the particle radius, ρ_P is the particle's density, R is the particle's external radius and $C_{i,bulk}$ is the bulk concentration of the i-th species.

The effectiveness factor is calculated throughout the expression in equation 4.19.

$$\eta_4 = \frac{4\pi R_P^2 D_{eff,j}\left(-\left.\frac{dC_j}{dr}\right|_{r=R_P}\right)}{\frac{4}{3}\pi R_P^3 r_4} \qquad 4.19$$

Where R_P is the catalyst radius, and the subscript j represents the j-th species. It was found for the present operation conditions that the value of η_4 assumes the value close to the one along the whole reactor, therefore, for the sake of simplicity of the modeling and for the utilization of less computational resources, a value equal to one was chosen as the effectiveness factor η_4.

4.2.2 Operational conditions for direct dimethyl ether

In Table 4-2 are reported the operational conditions for the direct dimethyl synthesis reactor.

Table 4-2 Operational conditions for direct dimethyl ether synthesis

Feed's molar fractions	CO	0.17
	CO_2	0.0404
	H_2	0.4282
	H_2O	0.0002
	CH_3OH	0.003
	DME	0.0018
	N_2	0.3129
	CH_4	0.0435
Pressure	5	MPa
Flash temperature	313.0	K
Flash pressure	7.5	MPa

The previous operational conditions were based on the work done by Song et al., 2008 [48] and Vakili & Eslamlouyean, 2012 [53].

4.3 Numerical aspects

The previous model was implemented on a Visual C++ 9.0 routine, the GaC reactor is characterized by the existence of a countercurrent flow of fresh inlet syngas that act as refrigerant for the reacting gas on the tube side of the reactor. As a result, a boundary value problem (BVP) is obtained. In it, the inlet temperature of the WaC reactor is unknown and the temperature of the feed synthesis gas entering the GaC is known (boundary condition).

In order to solve such system, a shooting method was implemented so the BVP is turned into an initial value problem (IVP) in which the temperature of the gas entering the WaC reactor is estimated and the ordinary differential equation (ODE) model is solved. Afterwards, the temperature of the feed synthesis gas is obtained and compared with the actual value and the process is repeated until reaching an acceptable tolerance.

On the other hand, the convergence path relating to the recycle loop has to be found, for this purpose, a method of successive substitution was used as described by Towler & Sinnott, 2007 [51] and Seider, Seader & Lewin, 2010 [45]; therefore, once the composition of the gas leaving the reactor is known the flash separator model is solved and part of the vapor fraction is recycled back to the reactor, consequently, the reactor model must be solved again with the new inlet composition using the process previously described. The new composition is compared with the one already obtained and the procedure is repeated until the following condition is satisfied:

$$abs\left(\frac{recycle_{cal} - recycle}{recycle}\right) \leq \varepsilon_{tol} \qquad 4.20$$

The *BzzMath 6.0* library [7] was used to solve the ODE system as well as the nonlinear system of equation derived from the shooting method.

It is worth noting that the abovementioned procedure was used for both the methanol synthesis simulations and for the direct dimethyl ether synthesis simulation.

4.4 Steady state simulation profiles

4.4.1 Methanol synthesis

In order to illustrate a temperature and molar fractions of the species profile along the reactor, the results of a steady state simulations are reported below, such simulation was carried out assuming a WaC/GaC length ratio equals to 0.7/0.3, WaC's shell temperature equals to 524 K and inlet feed temperature equals to 484 K, such values are typical operating conditions for the Lurgi type reactor according to Fatemeh et al. and Rahimpour [4,44].

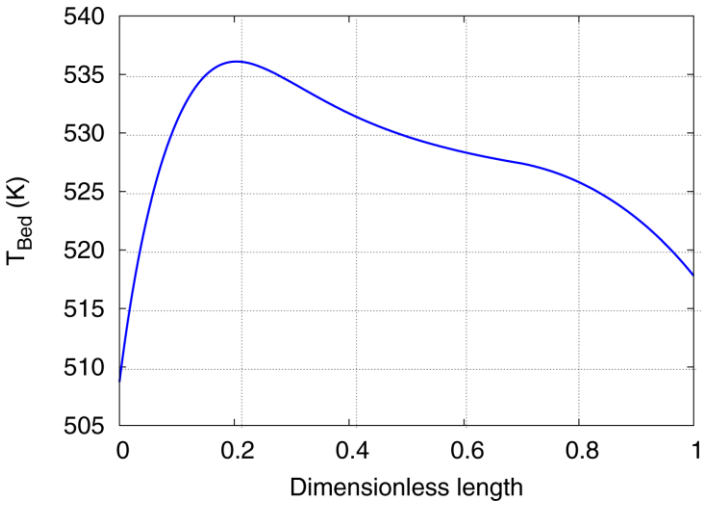

Figure 4-2 Temperature profile of tube side along the dual stage MeOH synthesis reactor.

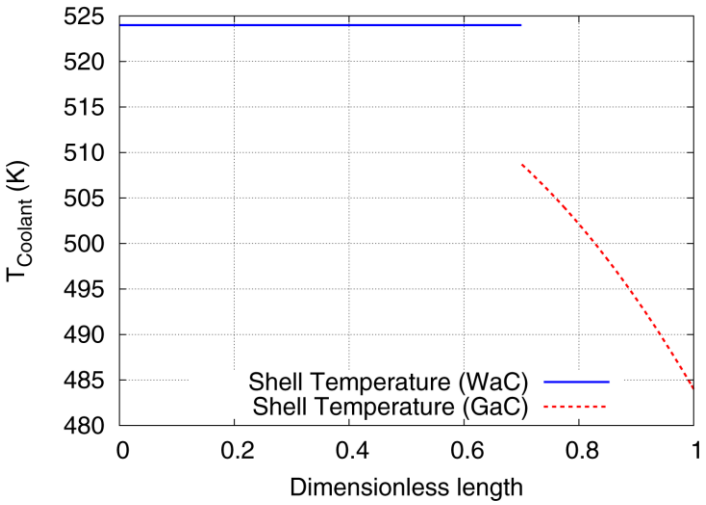

Figure 4-3 Temperature profile of shell side along the dual stage MeOH synthesis reactor.

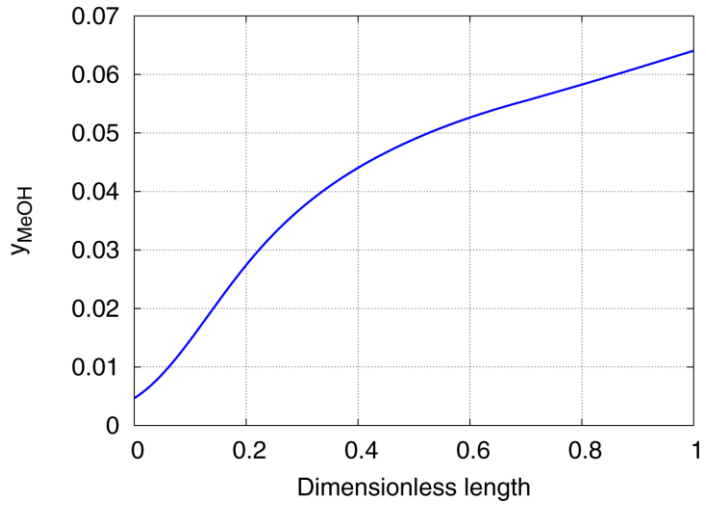

Figure 4-4 Methanol mole fraction profile along the dual stage MeOH synthesis reactor.

It can be observed from the temperature profile on Figure 4-2, that the first stage of the reactor (corresponding to the WaC reactor) is characterized by a steep increase of the temperature up until arriving to a hot spot around 1.3 - 1.4 m which is then followed by a slight decrease of temperature up to the limit of the WaC reactor. This behavior is attributed to the fact that in this stage the reaction is controlled kinetically, thus as the reaction is initiated thanks to heat provided by the water present in the shell side the temperature of the gas mixture is further increased by the exothermicity of the reaction and as a result the kinetic is favored producing methanol as shown in Figure 4-4 and specifically by the sharp increase in the methanol's molar fraction in this stage.

As the reaction system evolves, the thermodynamic equilibrium becomes more important severely limiting the reaction extent, this condition characterizes the later stage of the reactor system (corresponding to the GaC reactor). As can be noticed in Figure 4-2, the temperature of the gas mixtures decreases as it is used to heat the inlet syngas (Figure 4-3) something that is thermodynamically favorable for an exothermic reaction, on the other hand methanol's molar fraction slightly increases as the system reaches equilibrium.

4.5 Methanol Synthesis: sensitivity analysis

A sensitivity analysis was done on the following variables: WaC/GaC length ratio, shell side temperature of the WaC reactor (otherwise steam temperature) and feed's inlet temperature, such variables were those subject to optimization as will be observed in the following chapter.

4.5.1 Variation of WaC/GaC length ratio

From Figure 4-5 to Figure 4-8, are reported the profiles of the tube side temperature, shell side temperature and methanol mole fraction along the reactor for different values of WaC/GaC length ratio (LR).

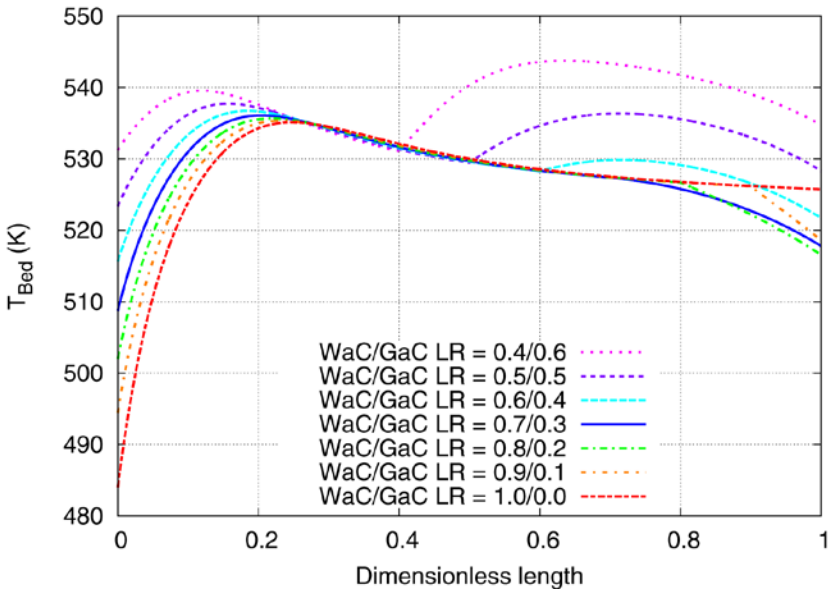

Figure 4-5 Temperature profile of tube side for different values of WaC/GaC length ratio (MeOH synthesis).

It can be observed from Figure 4-5 that for small values of WaC/GaC length ratio the temperature of the hot spot (tube side) in the WaC portion of the reactor is higher, this is due to the higher inlet temperature of the WaC reactor as the GaC portion increases for small values of length ratio, therefore, allowing to further heat the fresh inlet feed. Additionally, as was already explained in the WaC stage the reaction is controlled kinetically, nonetheless as long as the WaC /GaC length ratio decreases such kinetic control will continue to be active in the GaC stage producing a second hot spot in this portion. It can be noted that in such cases the temperature profile (bell type curve) of the GaC stage is characterized for being wider than that of the WaC reactor as the overall heat transfer coefficient is smaller. Moreover, for the case of length ratio equals to 0.4/0.6 the hot spot of the GaC stage is higher than that of the WaC portion and too close to the values of temperature where the catalyst suffers permanent damage.

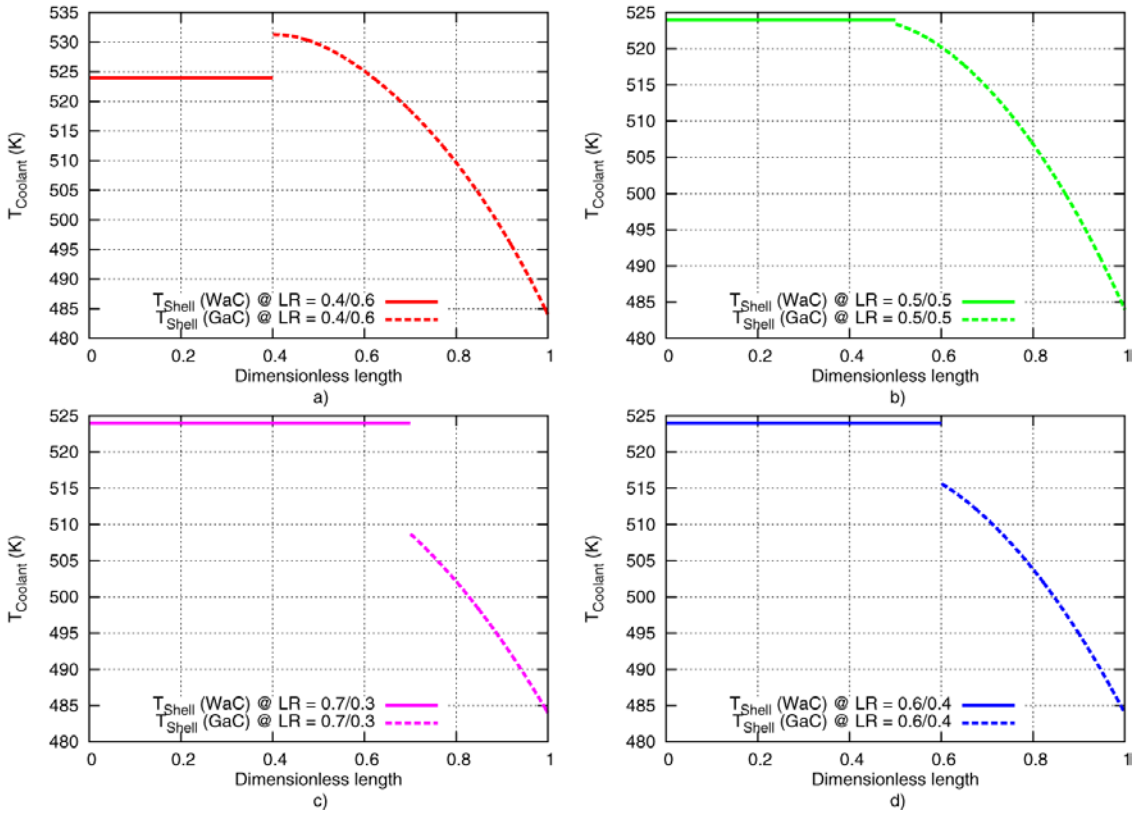

Figure 4-6 Comparison between shell side temperature profiles for a) LR = 0.4/0.6, b) LR = 0.5/0.5, c) LR = 0.7/0.3 and d) LR =0.6/0.4 (MeOH synthesis).

In Figure 4-6 and Figure 4-7 are plotted the profiles of the coolant temperature along the reactor, as explained before the highest inlet temperature of the WaC reactor correspond to the lower WaC/GaC length ratio (see Figure 4-6a). Finally, the extreme case is represented by the absence of the GaC stage where the tube side temperature approximates asymptotically (see Figure 4-5) to the coolants temperature that is constant along the reactor as seen in Figure 4-7a.

The profile of methanol mole fraction along the reactor is illustrated in Figure 4-8, as expected, for small values of WaC/GaC length ratio the outlet molar fraction is greater due to a higher tube temperature in both the WaC and GaC stages that enhances the rate of reaction as both portions act as kinetically controlled.

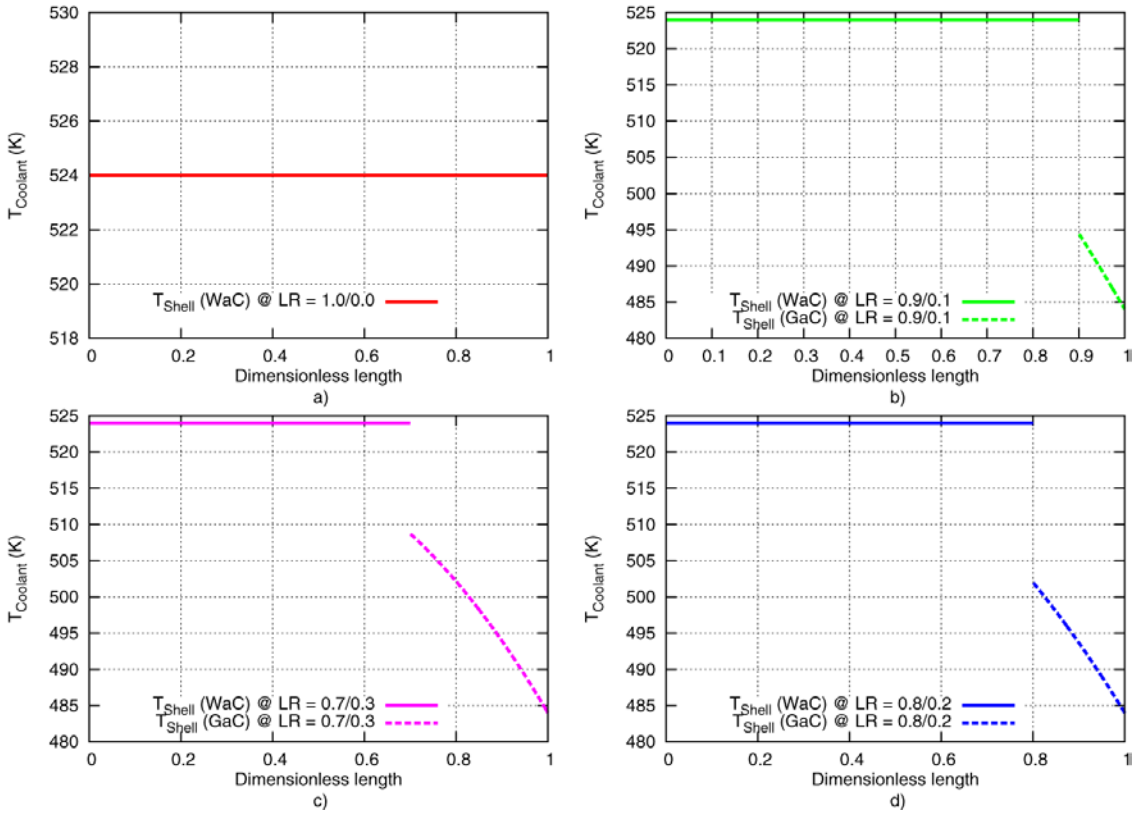

Figure 4-7 Comparison between shell side temperature profiles for a) LR = 1.0/0.0, b) LR = 0.9/0.1, c) LR = 0.7/0.3 and d) LR =0.8/0.2 (MeOH synthesis).

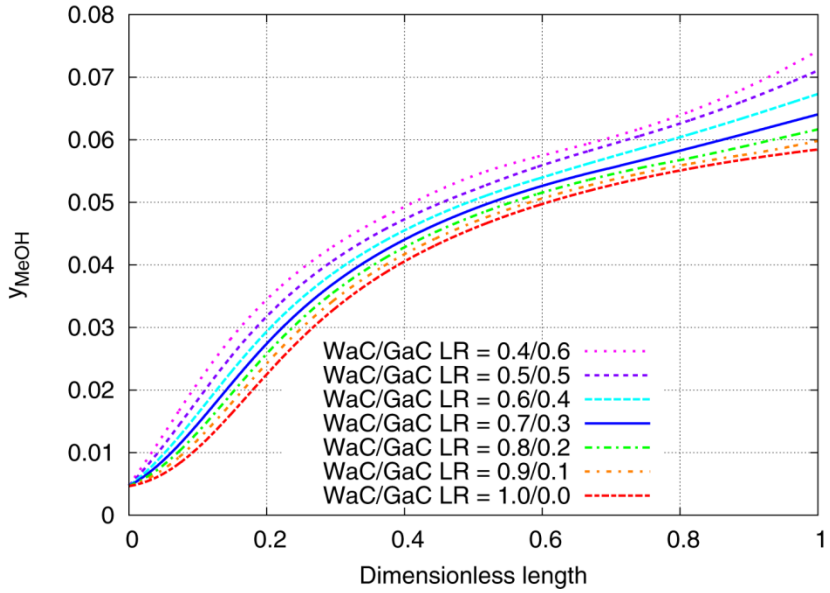

Figure 4-8 Methanol mole fraction profile along the reactor for different values of WaC/GaC length ratio (MeOH synthesis).

4.5.2 Variation of WaC's shell side temperature

From Figure 4-9 to Figure 4-12, the profiles of tube side temperature, shell side temperature and methanol mole fraction are presented for different values of the WaC's shell temperature or steam temperature.

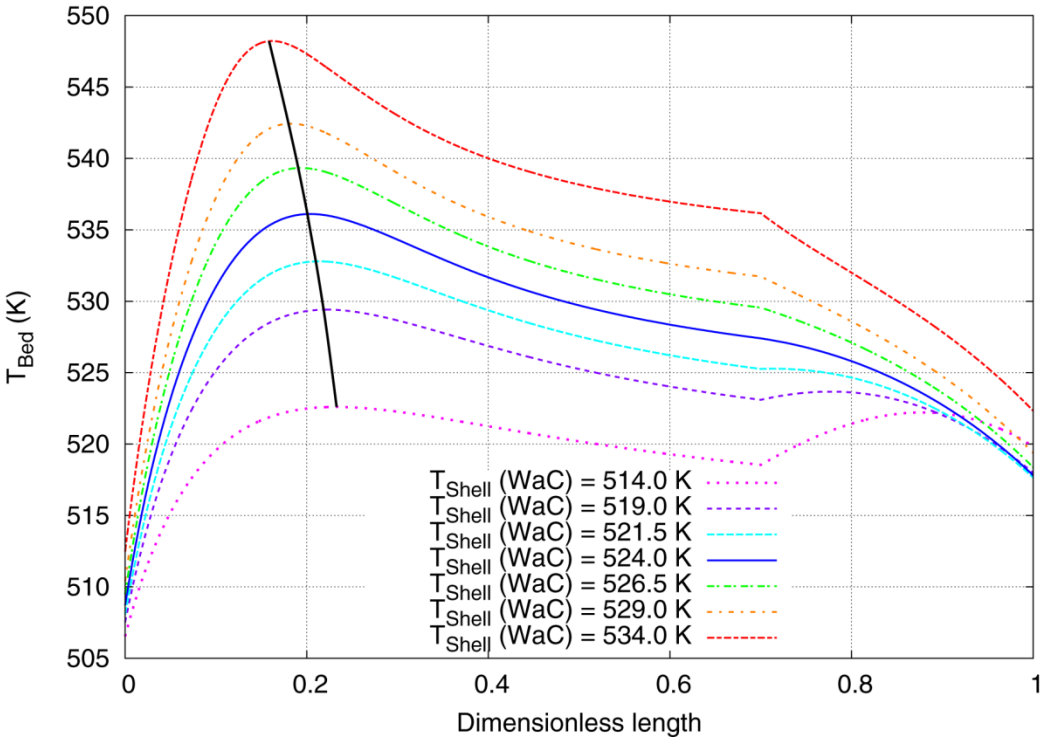

Figure 4-9 Temperature profile of tube side for different values of WaC's shell side temperature (MeOH synthesis).

The profile of the tube side temperature is shown in Figure 4-9, as expected, due to the exothermicity of the reaction higher temperatures in the WaC section are obtained for higher values of steam temperature, this is also assisted by a higher rate of reaction thanks to the kinetic control present in this stage as already discussed. It can also be noted that for lower steam temperatures a second hot spot in the GaC stage is present as the reaction has not approached equilibrium in the first stage and the kinetic control is still active in this latter stage.

In Figure 4-10 and Figure 4-11 it can be observed that the syngas feed, which acts as the coolant in the GaC section, leaves the second stage at higher temperatures for higher values of steam temperature, this is due to the fact that at such values the reacting gas enters the GaC stage at higher temperatures (see Figure 4-9). Such effect is similar to the one reported in the length ratio sensitivity analysis but with a reduced impact.

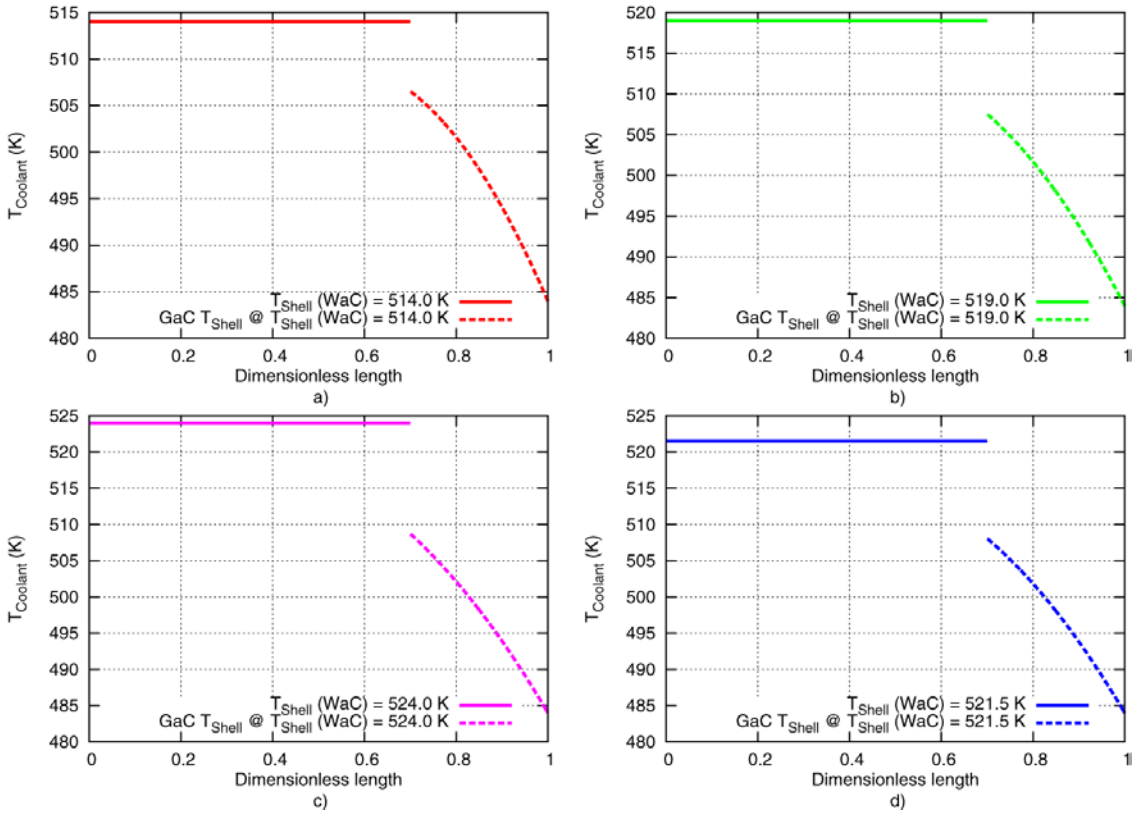

Figure 4-10 Comparison between shell side temperature profiles for values of WaC's shell's temperature equals to a) 514 K b) 519 K, c) 524 K and d) 521.5 K (MeOH synthesis).

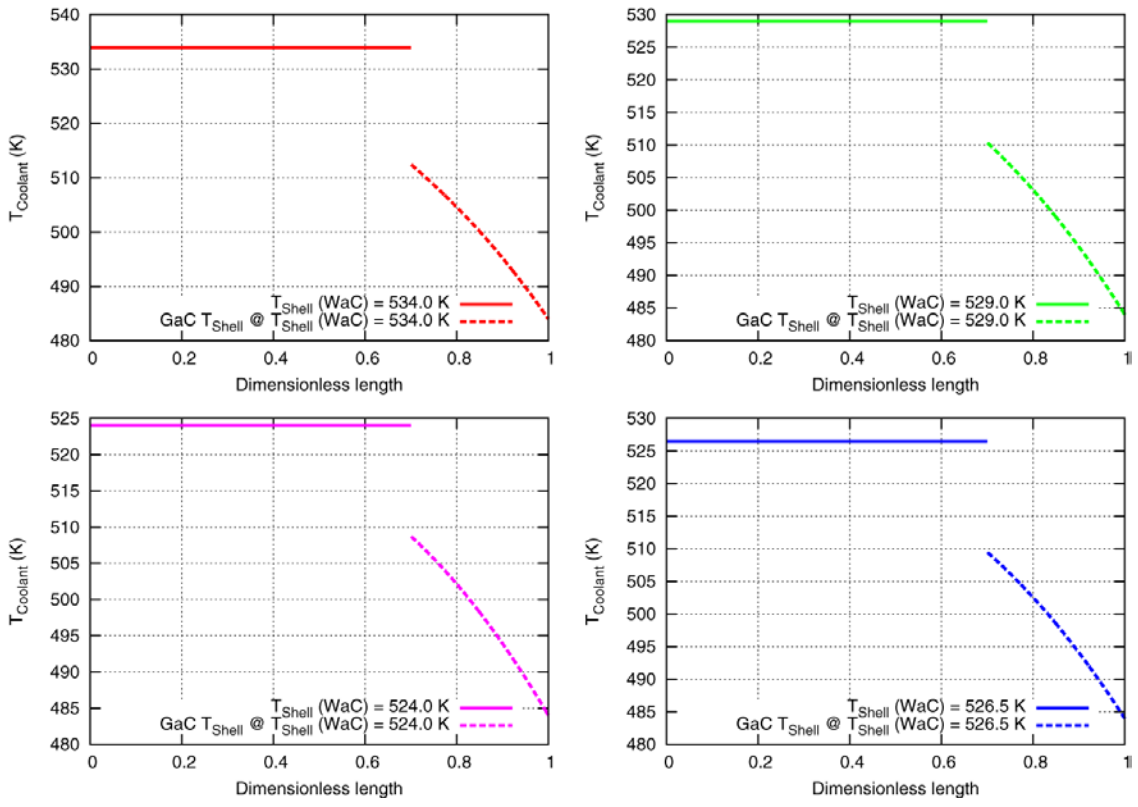

Figure 4-11 Comparison between shell side temperature profiles for values of WaC's shell's temperature equals to a) 534 K b) 529 K, c) 524 K and d) 526.5 K (MeOH synthesis).

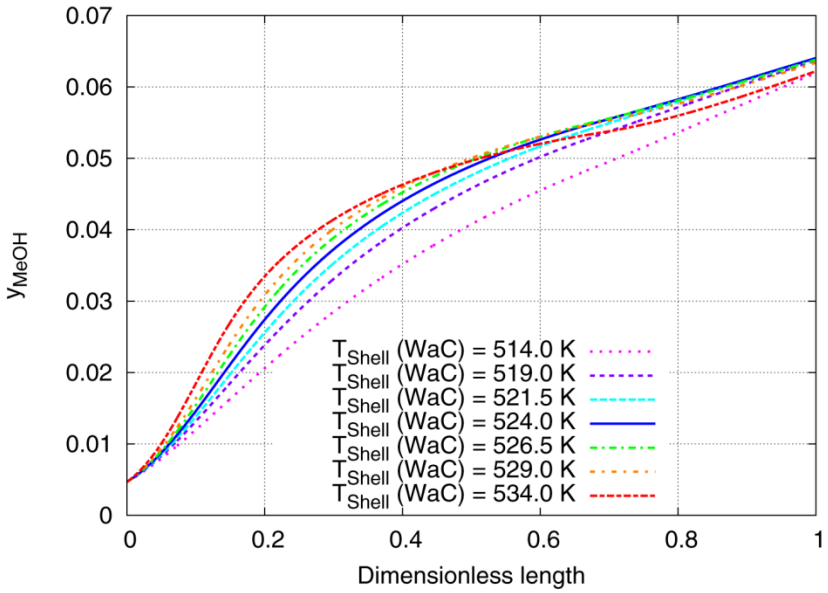

Figure 4-12 Methanol mole fraction profile along the reactor with different values of WaC's shell side temperature (MeOH synthesis).

It can be seen from Figure 4-12 that the outlet methanol mole fraction is not affected in a greater extent in neither of the studied cases, the only noticeable effect is present in the first portion of the WaC reactor where the methanol mole fraction is more developed for high values of steam temperature. Nonetheless, as can be observed for the case of steam temperature equals to 534 K, entering the second stage at high temperatures is a drawback as the GaC stage is equilibrium controlled and higher temperatures are detrimental to exothermic reaction's equilibrium, as a result, the outlet methanol mole fraction is slightly lower when compared to the other cases.

4.5.3 Variation of inlet's feed temperature

From Figure 4-13 to Figure 4-16, the profiles of tube side temperature, shell side temperature and methanol mole fraction were obtained for different values of the feed's inlet temperature.

As observed in Figure 4-13 the WaC's temperature profile is not significantly affected by the inlet's feed temperature as the effect is extended solely to the WaC's inlet temperature, thus, the hot spot position is slightly higher and shifted to the left in a lesser extent as the feed temperature increases. In contrast, the effect is considerable in the GaC stage as increasing the inlet's feed temperature decreases the cooling capacity of this stage while increasing the outlet temperature of the dual stage reactor.

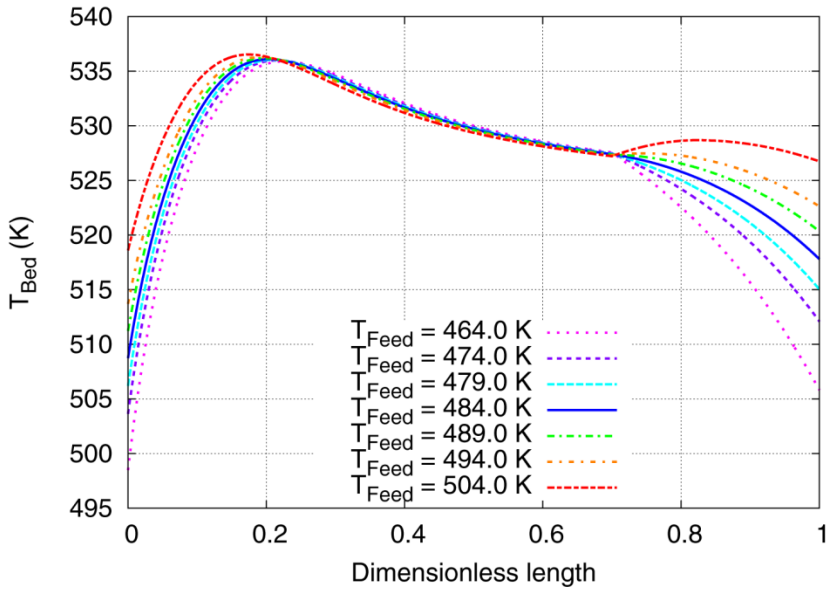

Figure 4-13 Temperature profile of tube side with different values of feed's inlet temperature (MeOH synthesis).

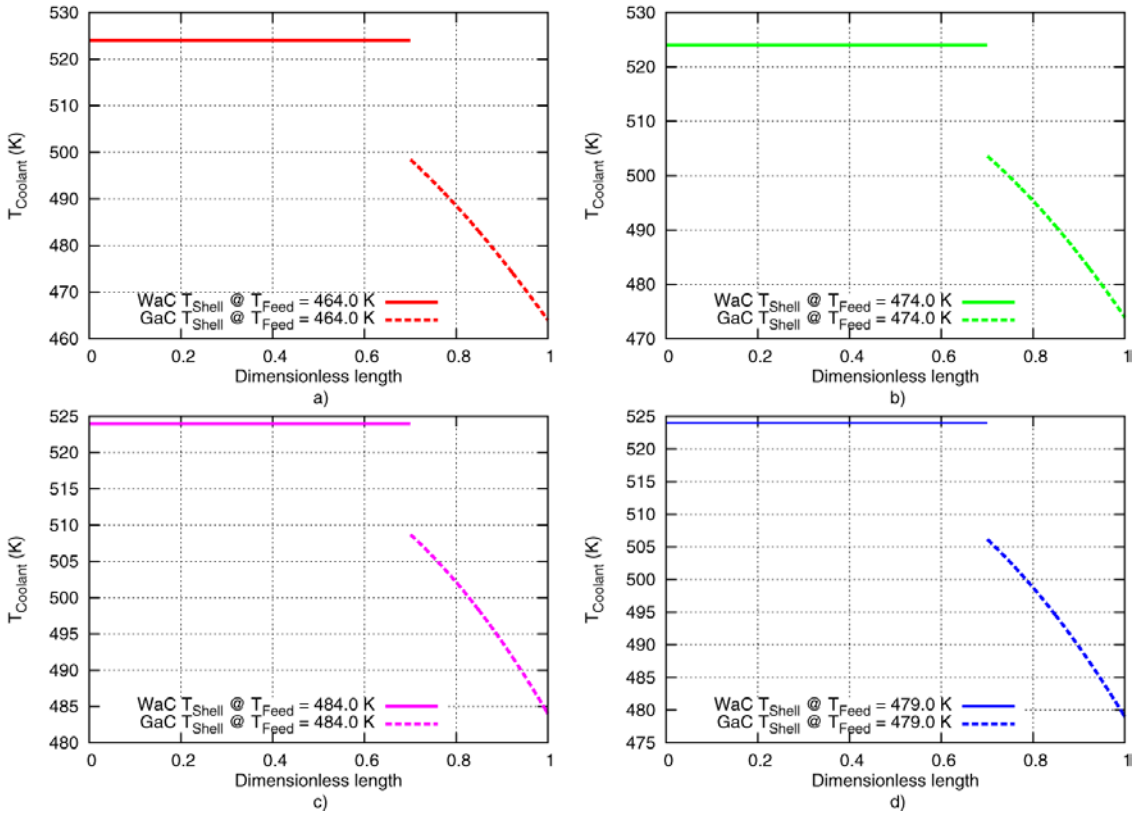

Figure 4-14 Comparison between shell side temperature profiles with values of feed temperature equals to a) 464 K b) 474 K, c) 484 K and d) 479 K (MeOH synthesis).

As already explained the most noticeable effect of the inlets feed temperature variation is the variation in the WaC's inlet temperature as seen in Figure 4-14 and Figure 4-15.

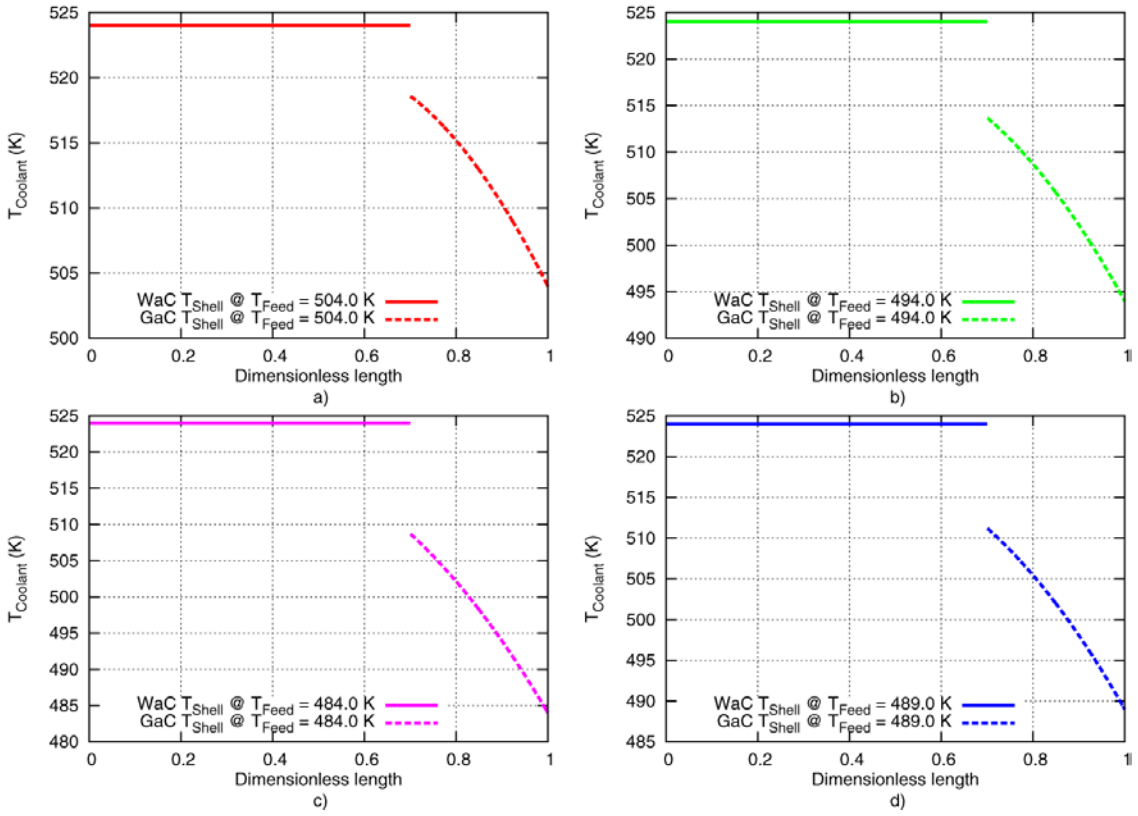

Figure 4-15 Comparison between shell side temperature profiles with values of feed temperature equals to a) 504 K b) 494 K, c) 484 K and d) 489 K (MeOH synthesis).

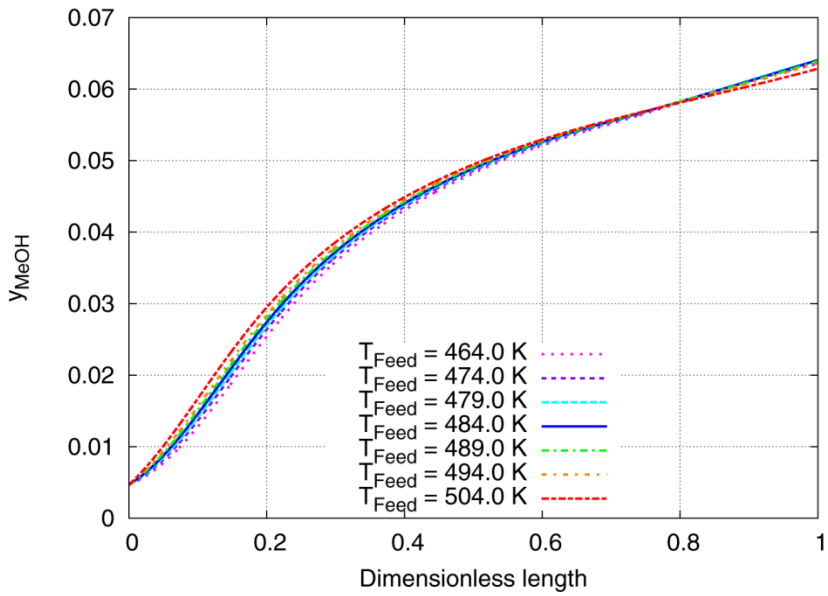

Figure 4-16 Methanol's molar fraction profile with different values of feed's inlet temperature (MeOH synthesis).

Finally, from Figure 4-16 it can be seen that the effect of inlet's feed temperature is not significant in the methanol mole fraction as its value slightly changes along the reactor. Again, for high values of the outlet temperature in the tube side, resulting from a higher

inlet's feed temperature, the outlet methanol mole fraction is slightly lower than in any of the other cases confirming the detrimental effect of the thermodynamic equilibrium that characterize the methanol synthesis reaction.

4.6 Dimethyl ether synthesis: steady state simulation profiles

Literature on the modeling and simulation of direct dimethyl ether synthesis is quite recent as such topic is still on development thanks to the renovated interest on the utilization of dimethyl ether as an alternative fuel. The most relevant literature is summarized in few papers by Vakili & Eslamlouyean, 2012 [53]; Song et al., 2008 [48]; and McBride, Turek and Güttel, 2012 [36]. It is worth noting that not all of these works consider the dual stage reactor and/or employ different kinetic models in their studies.

As literature references for the direct synthesis of dimethyl ether in a dual stage reactor is poor a base case could not be defined, as a result, a sensitivity analysis was directly made assuming almost the same configuration of the dual stage methanol synthesis reactor, the most relevant modification was in the reactor's tube inside and outside diameter (from 0.0341 m to 0.046 m and from 0.0381 m to 0.05 m respectively) and the WaC's shell temperature and according to the work of Vakili & Eslamlouyean, 2012 [53]. In the methanol's sensitivity analysis it was possible to appreciate that the influence of the inlet's feed temperature is not significant for the behavior of the overall reactor network and similarly, it will not be considered in the sensitivity analysis of the direct dimethyl ether synthesis. Conversely, since there are no prior studies and detailed analysis on the feed's molar flow to the reactor, this variable will be included in the sensitivity analysis and, then, in the successive optimization.

4.7 Dimethyl ether synthesis: sensitivity analysis

4.7.1 Variation of WaC/GaC length ratio

A similar tendency to the MeOH sensitivity analysis for the tube side temperature was obtained as seen in Figure 4-17, once again as the GaC reactor becomes longer the WaC's inlet temperature is higher due to an improved heating of the inlet feed gas. Such effect is also possible to observe in Figure 4-18 and Figure 4-19 where high outlet feed temperatures are (first point of the dashed line) achieved for longer GaC portions in the reactor.

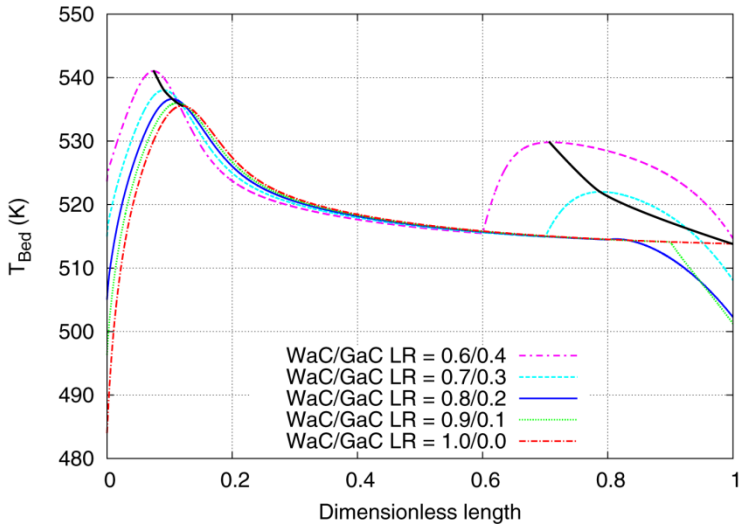

Figure 4-17 Temperature profile of tube side for different values of WaC/GaC length ratio (direct DME synthesis).

It can be noted that the bell shape of the WaC's tube temperature is narrower than the one of the MeOH synthesis; this is due to the higher exothermicity of the direct dimethyl ether synthesis reaction that produces a steeper increase in temperature. Therefore, noting that the bifunctional catalyst is composed in part of $CuO/ZnO/Al_2O_3$ which is susceptible to sintering, the control of temperature profile and especially of the temperature of the hot-spot is critical in order to avoid the deactivation of the metallic part of the catalyst.

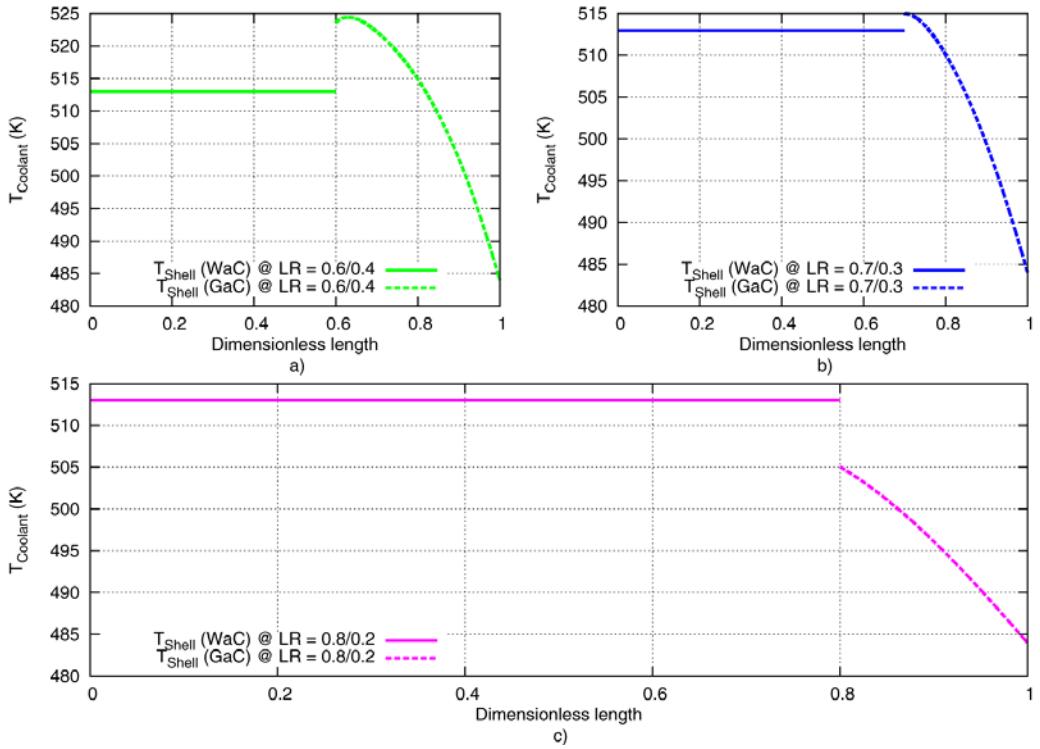

Figure 4-18 Comparison between shell side temperature profiles for a) LR = 0.6/0.4, b) LR = 0.7/0.3 and c) LR = 0.8/0.2 (direct DME synthesis).

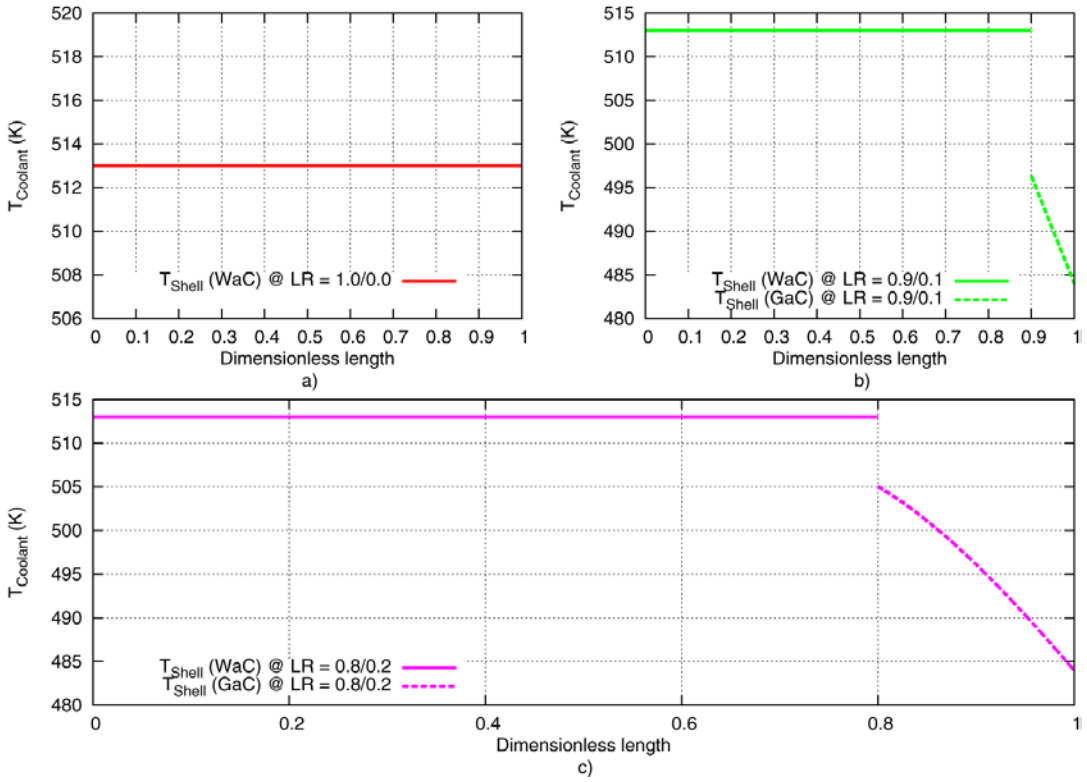

Figure 4-19 Comparison between shell side temperature profiles for a) LR = 1.0/0.0, b) LR = 0.9/0.1 and c) LR = 0.8/0.2 (direct DME synthesis).

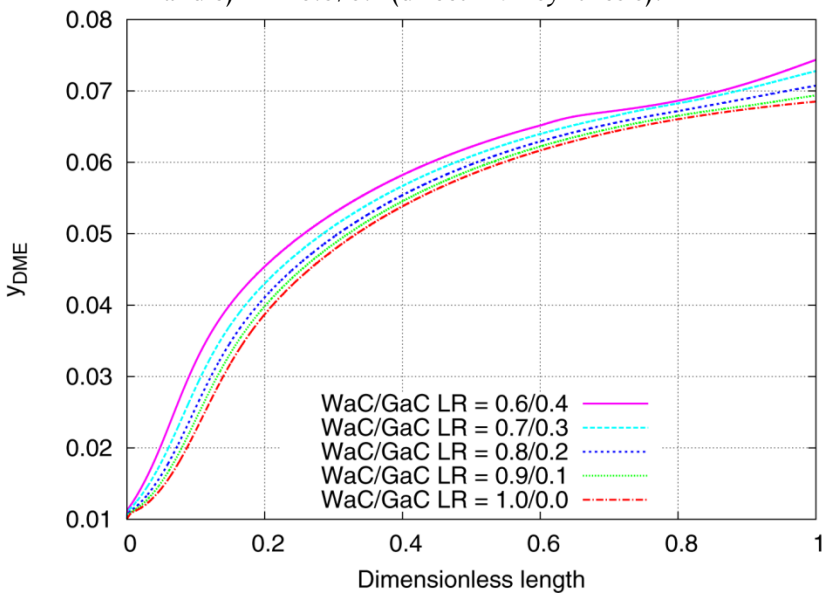

Figure 4-20 Dimethyl ether mole fraction profile along the reactor for different values of WaC/GaC length ratio (direct DME synthesis).

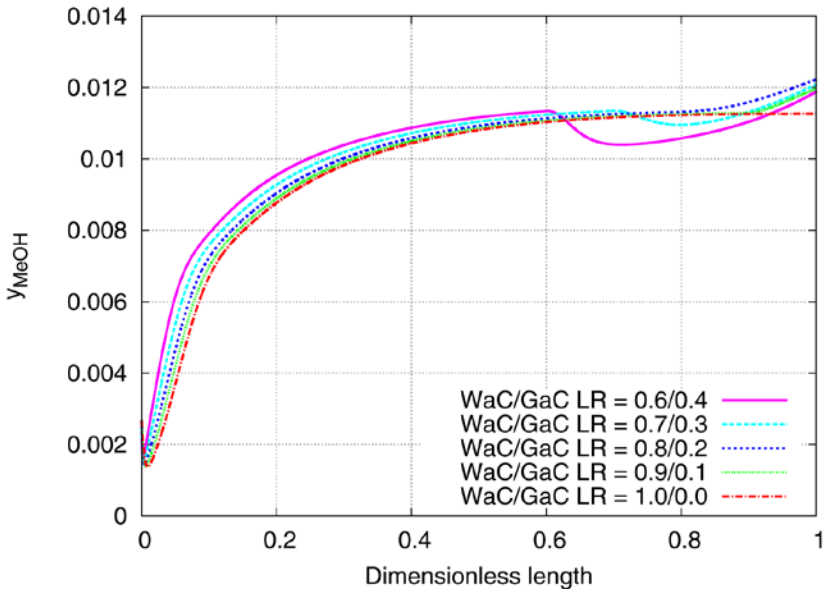

Figure 4-21 Methanol mole fraction profile along the reactor for different values of WaC/GaC length ratio (direct DME synthesis).

Once again as higher temperatures are adopted for lower values of WaC/GaC length ratio higher fractions of DME are obtained as illustrated in Figure 4-20. It is worth noting that the scientific community agrees with the fact that the dimethyl ether synthesis process is kinetically controlled [28] and therefore the effect of thermodynamic equilibrium is not as unfavorable as for the methanol synthesis. Actually, this unfavorable effect can still be observed in Figure 4-21 where for the cases in which a second hot spot is developed (WaC/GaC = 0.6/0.4 and 0.7/0.3) the methanol fraction decreases due to the detrimental effect of high temperature in reactors where exothermic reactions take place.

4.7.2 Variation of WaC's shell side temperature

From Figure 4-22 it is possible to observe that a similar trend to the methanol synthesis was obtained, consequently, as the WaC stage is kinetically controlled, increasing the temperature of the boiling water unavoidably means to enhance the kinetics and therefore the temperature rises thanks to the exothermicity of the reaction. Additionally, the hot spot is higher in comparison with the methanol synthesis reaction as it is less exothermic.

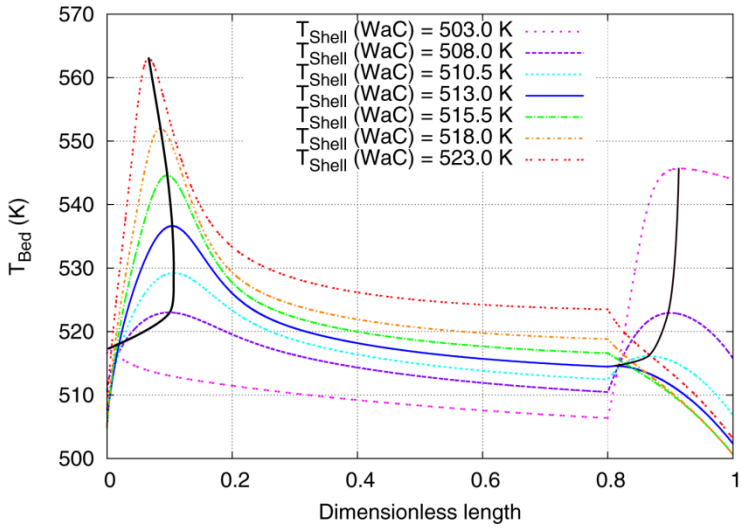

Figure 4-22 Temperature profile of tube side for different values of WaC/GaC length ratio (direct DME synthesis).

On the other hand, for low values of steam temperature a second hot spot is present as expected, the reason for this is that low temperatures deteriorates the kinetics of reaction and therefore the kinetic control that characterizes the WaC stage of the reactor is still important in the GaC reactor and as the overall heat transfer coefficient is lower in such stage, the reaction is able to kinetically develop in this stage.

In contrast, from Figure 4-23 and Figure 4-24 the methanol and dimethyl ether mole fractions path are enhanced for high values of steam temperature thanks to the favorable reaction kinetics, nonetheless, the outlet dimethyl ether mole fraction is not affected as enhanced due to the equilibrium limitations.

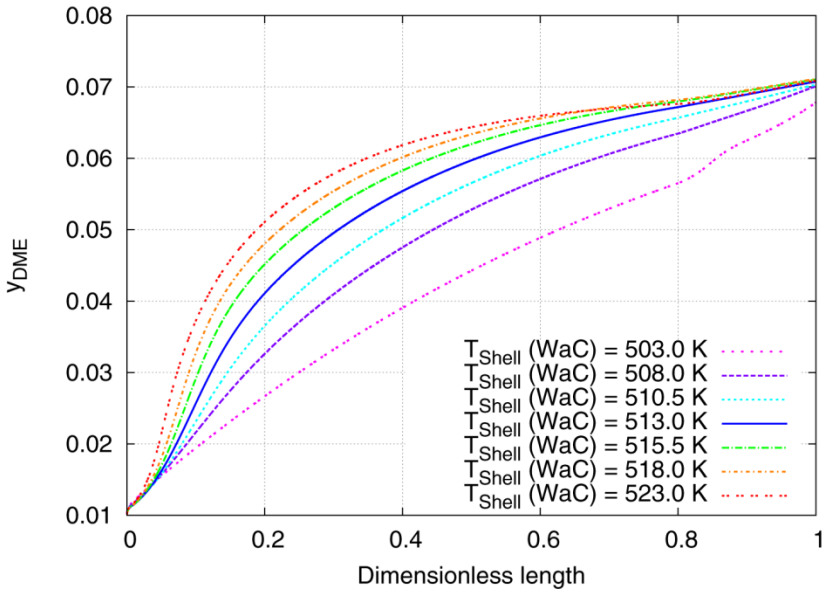

Figure 4-23 Dimethyl ether mole fraction profile along the reactor for different values of WaC/GaC length ratio (direct DME synthesis).

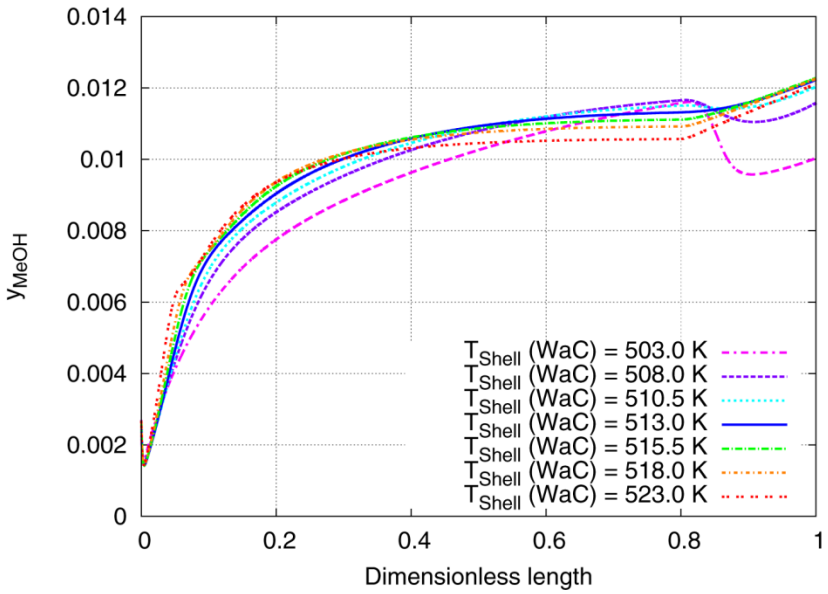

Figure 4-24 Methanol mole fraction profile along the reactor for different values of WaC/GaC length ratio (direct DME synthesis).

Finally, it is possible to see from Figure 4-24 the effect of the second hot spot on methanol mole fraction, it can be observed that low shell temperature in the WaC reactor deactivates the kinetics of reaction in this stage allowing the reaction to be active in the GaC that reaches high tube side temperatures due to a lower overall heat transfer coefficient, as a result of this, the methanol fraction decreases sharply thanks to an unfavorable the equilibrium thermodynamics of methanol synthesis for high temperatures.

4.7.3 Variation of feed's molar flow

Variation of feed inlet flow was introduced in the direct dimethyl ether synthesis study as there is poor data in this process and specially when dealing with the dual stage fixed bed reactor.

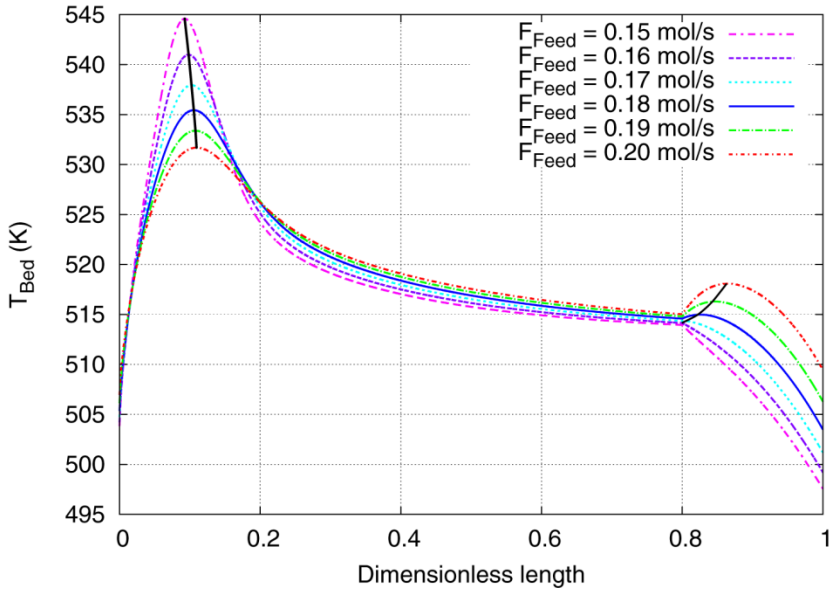

Figure 4-25 Temperature profile of tube side for different values of feed's molar flow (direct DME synthesis).

The tube side temperature profile for different values of feed's molar flow is presented in Figure 4-25, it can be noticed that low values of feed's molar flow present higher temperatures in the hot spot as this implies longer residence times and therefore longer contact between the reacting gas and the catalyst favoring the overall reaction. Nonetheless, low values of feed's molar flow introduce drawbacks for the catalyst service life as it can increase the deactivation of the metallic portion of the bifunctional catalyst.

Additionally, it is observed that the cooling capacity of the GaC stage of the reactor is lower as additional heat from the reaction is produced when feed's molar flow increases. This could allow to an efficiently use of the GaC stage of the reactor allowing the reaction to be further developed in such stage increasing the production of DME and MeOH, the conversion of syngas while maintaining safe operating conditions to preserve the catalyst activity.

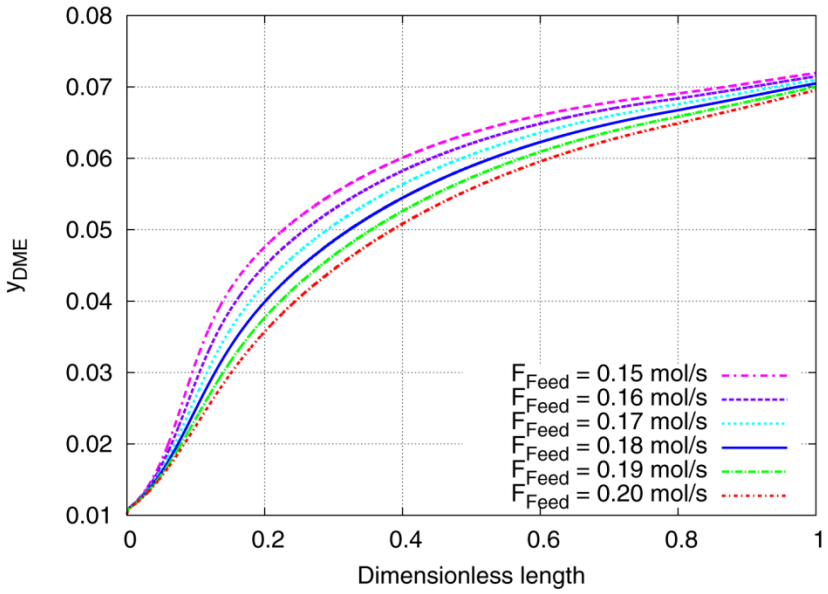

Figure 4-26 Dimethyl ether mole fraction profile along the reactor for different values of feed's molar flow (direct DME synthesis).

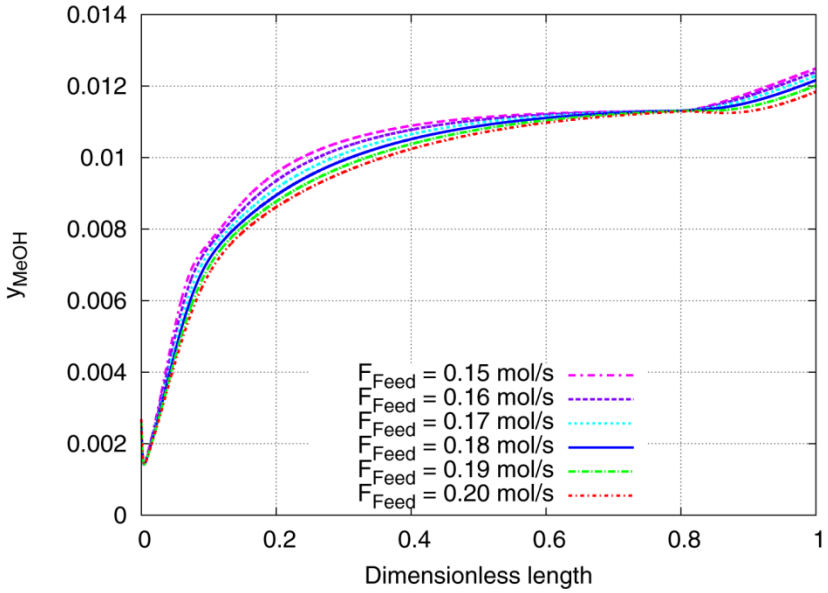

Figure 4-27 Methanol mole fraction profile along the reactor for different values of feed's molar flow (direct DME synthesis).

As expected, low values of feed's molar flow increase the production of dimethyl ether and methanol as seen in Figure 4-26 and Figure 4-27 thanks to an improved kinetics as tube side temperature is higher along the reactor. The detrimental effect of thermodynamic equilibrium in methanol synthesis can be appreciated while comparing both figures, it can be seen that for values of length ratio near to 0.8 the methanol mole fraction converge in a point regardless of the feed's molar flow, in contrast, the molar fraction of dimethyl ether keeps increasing without being affected by the equilibrium. This could indicate the advantages of the synergic effect of coupling both systems of reaction as dimethyl ether

production is not affected by any equilibrium limitation of the methanol synthesis reaction.

5. Process Design Results: Application of Systematic Staging

This chapter is devoted to the optimization of the methanol synthesis process and the direct dimethyl ether synthesis process as a part of the systematic staging design. An unconstrained minimization routine included in the *BzzMath* library will be employed, particularly, the *BzzMinimizationRobust* class.

5.1 Systematic staging design

As described before, the systematic staging design of Hillestad, 2010 [26] was employed in reviewing the staged design of both methanol and direct dimethyl ether synthesis reactors. This methodology covers essentially a model formulation and an optimization procedure of the so-called reactor path that is defined as the line of production in which a series of functions or operations take place.

The model formulation applied is either a homogeneous or a pseudo-heterogeneous model employing a plug flow, a CSTR reactor or a combination of both through the utilization of a design function that will be explained later. The complexity of such model can be increased by considering internal or external mass transfer limitations.

Five basic operations are considered and they are fluid mixing; chemical reaction; heat exchange; extra feeding and pressure change and each function can be divided furthermore in several specific design functions. Nonetheless, several other basic operations can be including depending of the complexity of the system.

The fluid mixing design function allows considering either the utilization of a plug flow reactor when there is mixing, a medium point equivalent to a plug flow reactor with recycling or lastly a CSTR when infinite recycle is considered. The chemical reaction

operation includes design functions to consider catalyst dilution and the employment of different catalyst. The heat exchange operation considers different exchange area distribution and different temperatures of coolant. The extra feeding operation extends the model through while contemplating a feed distribution and different composition and/or temperature of the feed. Finally, pressure change includes a design function to specify a pressure profile.

The present work is intended to the review of current technologies and as a result, the fluid mixing operation is not considered as such technologies are based on the utilization of plug flow reactors. On the other hand, extra feeding operations and pressure change operations are out of the scope of this work and will not be considered either. Accordingly to this, the functions considered are the utilization of different catalyst types, different exchange area distribution, and different coolant temperature.

The optimization procedure is intended to the maximization of one or several objective functions that are usually economical and are leaded toward the increase of productivity and energy efficiency. Additionally, the cost derived from the complexity of the design can also be considered. The optimal problem also includes one or several non-linear inequality constraints, so heuristics play a major role in the formulation.

The solution of such optimization problem is made using the Pontryagin maximum principle parameterizing the design function and state variables in order to account for constraints along the reactor path. However, as already explained, this work will employ the *BzzMinimizationRobust* class a powerful optimization tool included in the *BzzMath* library.

5.2 BzzMath library minimization class

The BzzMath is a comprehensive numerical library entirely written in C++ adopting an object-oriented programming and is freely available at Professor Buzzi-Ferraris homepage (see Ref. [7]); the library covers several topics in numerical analysis such as differential systems, linear algebra, non-linear systems and others.

As explained in Buzzi-Ferraris & Manenti, 2013 [9] the *BzzMinimizationRobust* class employs the OPTNOV-Simplex hybrid method.

5.2.1 Nelder & Mead simplex method

The simplex method was originally proposed by Spendley, Hext & Himsworth, 1962 [49] and was subsequently improved and modified by Nelder & Mead, 1965 [40]. In this method, a set of $N+1$ (with $N = n_v$) different vertices $\boldsymbol{v}_0, \boldsymbol{v}_1, \dots, \boldsymbol{v}_{N-1}, \boldsymbol{v}_N$ is called the simplex.

Vertices are sorted to have increasing function values with respect to the index of vertices: $\mathrm{F}_0 \leq F_1 \leq \cdots \leq F_{N-1} \leq F_N$. The vertex $\boldsymbol{v}_0$ contains the best value and $\boldsymbol{v}_N$ the worst value of the $N+1$ vertices.
The barycenter $\boldsymbol{v}_B$ of the vertices from 0 to $N-1$ is calculated through the arithmetic mean of their coordinates by excluding the worst vertex $\boldsymbol{v}_N$.

The method is based on three fundamental operations: *reflection*, *expansion*, and *contraction*. Given $N+1$ distinct initial vertices, the new vertex $\boldsymbol{v}_R$ is obtained by reflecting the worst vertex $\boldsymbol{v}_N$ with respect to the barycenter $\boldsymbol{v}_B$:

$$\boldsymbol{v}_R = \boldsymbol{v}_B + \alpha(\boldsymbol{v}_B - \boldsymbol{v}_N) \quad \alpha > 0 \qquad 5.1$$

The following cases may occur:
1) The function in $\boldsymbol{v}_R$ is better than $\boldsymbol{v}_0$.
In such a case, the reflection is to be expanded:

$$\boldsymbol{v}_R = \boldsymbol{v}_B + \gamma(\boldsymbol{v}_R - \boldsymbol{v}_B) \quad \gamma > 1 \qquad 5.2$$

If $\mathrm{F}(\boldsymbol{v}_E) < \mathrm{F}(\boldsymbol{v}_R)$, the point $\boldsymbol{v}_E$ is introduced in the simplex by replacing $\boldsymbol{v}_N$ (the new vertices of the simplex are $\boldsymbol{v}_E, \boldsymbol{v}_1, \dots, \boldsymbol{v}_{N-1}, \boldsymbol{v}_N$).
On the other hand, if $\mathrm{F}(\boldsymbol{v}_E) > \mathrm{F}(\boldsymbol{v}_R)$, the point $\boldsymbol{v}_R$ is introduced in the simplex by replacing $\boldsymbol{v}_N$ (the new vertices of the simplex are $\boldsymbol{v}_R, \boldsymbol{v}_1, \dots, \boldsymbol{v}_{N-1}, \boldsymbol{v}_N$).

2) The vertex $\boldsymbol{v}_R$ is worse than $\boldsymbol{v}_0$ but better than $\boldsymbol{v}_{N-1}$: $\mathrm{F}_0 < \mathrm{F}_R < \mathrm{F}_{N-1} < F_N$. In such case $\boldsymbol{v}_R$ is introduced in the simplex by replacing $\boldsymbol{v}_N$ (the new vertices of the simplex are $\boldsymbol{v}_0, \dots, \boldsymbol{v}_R, \dots, \boldsymbol{v}_{N-1}$).

3) The vertex $\boldsymbol{v}_R$ is worse than $\boldsymbol{v}_0$, better than $\boldsymbol{v}_N$, but worse than $\boldsymbol{v}_{N-1}$: $\mathrm{F}_0 < \mathrm{F}_{N-1} < \mathrm{F}_R < F_N$. In this case, a contraction is performed:

$$\boldsymbol{v}_C = \boldsymbol{v}_B + \beta(\boldsymbol{v}_R - \boldsymbol{v}_B) \quad 0 < \beta < 1 \qquad 5.3$$

4) The vertex $\boldsymbol{v}_R$ is worse than $\boldsymbol{v}_N$: $\mathrm{F}_0 < \cdots < \mathrm{F}_N < F_R$. In this case, a contraction in the opposite direction (with respect to the previous reflection) is carried out:

$$\boldsymbol{v}_C = \boldsymbol{v}_B + \beta(\boldsymbol{v}_N - \boldsymbol{v}_B) \quad 0 < \beta < 1 \qquad 5.4$$

If the vertex $\boldsymbol{v}_C$ evaluated by means of (5.3) and (5.4) is better than $\boldsymbol{v}_N$, this is replaced by the same $\boldsymbol{v}_C$ and the new vertices of the simplex are $\boldsymbol{v}_0, \dots, \boldsymbol{v}_{N-1}, \boldsymbol{v}_C$ or $\boldsymbol{v}_0, \dots, \boldsymbol{v}_C, \dots, \boldsymbol{v}_{N-1}$. Otherwise the simplex is contracted in the neighborhood of the best vertex $\boldsymbol{v}_0$ by means of the formula:

$$\boldsymbol{v}_i = \boldsymbol{v}_i - \delta(\boldsymbol{v}_i - \boldsymbol{v}_0) \quad 0 < \delta < 1 \qquad 5.5$$

The values suggested by Nelder & Mead are: $\alpha = 1$, $\beta = 0.5$, $\gamma = 2$ and $\delta = 0.5$. The method continues while the distance of vertices $\boldsymbol{v}_i$ from $\boldsymbol{v}_0$ is larger than an assigned tolerance. Another stop criterion is to check that the function is not constant in all vertices of the simplex.

The Simplex method has the following pros and cons:

Pros:

- The objective function does not have any special requirements: in fact, it can be non-derivable and discontinuous.
- It solves relatively narrow valleys.
- It is a good method when coupled with more performing algorithms.

Cons:

- It does not allow the minimum to be detected with a high level of accuracy except after a large number of calculations.
- It requires a lot of memory allocation when the number of variables is large.
- The method can be used only for small- and medium-scale problems.
- In the presence of narrow valleys, the vertices may collapse in a sub-space. If this happens, the method is unable to find the function minimum.
- It does not exploit the function information obtained during the search: it is not high performance when the function is easy.

5.2.2 OPTNOV–Simplex hybrid method

Most traditional methods are ineffective especially when the function valleys are particularly narrow (see Figure 5-1). These methods perform one-dimensional searches along certain specific axes which are selected in accordance with the method used. When the valley is very narrow it can happen that none of the search axes result in any function improvement, even though it is reasonably oriented like the valley bottom. This is the typical case of chemical reaction engineering where the kinetic parameters are strongly unbalanced.

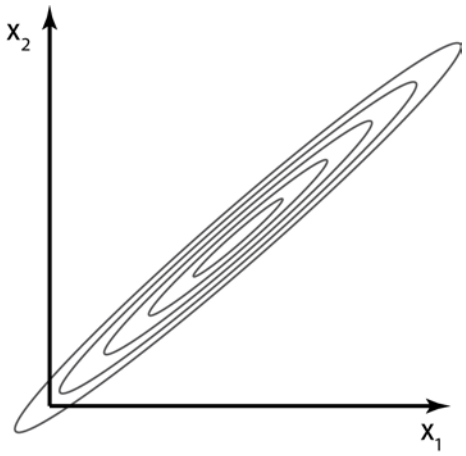

Figure 5-1 A qualitative example of a narrow valley for which traditional minimization methods are ineffective

Therefore, robust optimization methods are necessary in order to circumvent issues related with the following situations:

- The function is undefined in some regions and the domain cannot be described analytically;
- Very narrow valleys are present;
- The function is multimodal and the global optimum is required;
- The function and/or its derivatives are discontinuous
- The function cannot be approximated by a quadratic in correspondence with the optimum.

In order to overcome the previous limitation, the OPTNOV method is used. It was introduced by Buzzi-Ferraris, 1967 [8] and is based on the following ideas:

- Whatever optimization algorithm is able to find the bottom of the valley quickly by starting from a point outside the same valley.
- The line joining two points on the bottom of the valley is a reasonable valley direction; therefore there is a good probability than a point projected along such a direction will be close to the valley.
- Nevertheless, this valley direction must not be used as the direction of the one-dimensional search; rather it should be the direction along which a new point is projected.
- The new point projected in the valley direction should not be discarded even though it is worse than the previous one; it should be adopted as the new starting point in the search for the minimum.
- This search must be performed in the sub-space orthogonal to the valley direction to prevent the problem of small steps arising. In fact, if the axis is used to minimize the function (particularly when it is the first axis of search), it is possible to return to the previous point in one very small movement.

As a result, the OPTNOV method is adopted to improve the robustness of the Simplex method and is intended to iteratively select a new starting point which is used by the Simplex method with a limited number of iterations.

The OPTNOV-Simplex hybrid method has the following pros and cons:

Pros:

- The objective function does have any special requirements: in fact, it can be non-derivable and discontinuous, and no quadratic functions can reasonably approximate it in the optimum.
- It allows narrow valleys to be followed.
- The function can be undefined in some regions and the domain cannot be analytically described.

Cons:

- It is inefficient with respect to other alternatives when robustness is not necessary.
- The method can only be used for small- and medium-scale problems.

5.3 Methanol synthesis process design & optimization

The systematic design approach proposed by Hillestad, 2010 [26] intended for staged reactors was partially applied. As stated in the previous work, staging is not a new idea in reactor design and dividing a reactor into a finite number of stages provides additional degrees of freedom, as a result, each stage is designed in order to achieve an overall optimized objective.

Basing on the integrated model of the WaC/GaC reactor network, including separation and recycle, it is possible to optimise the methanol synthesis by selecting certain degrees of freedom. As already explained, two stages compose the methanol synthesis reactor network, one is the water-cooled stage (WaC) and the other is the gas-cooled stage (GaC) and the design of the synthesis reactor (and its stages) was approached throughout the following three cases:

- 1st case: monodimensional optimization of the WaC/GaC length ratio was carried out with the objective of maximizing methanol mole fraction (Monodimensional process optimization).
- 2nd case: monodimensional optimization of the WaC/GaC length ratio with the objective of maximizing methanol mole fraction and steam generation (monodimensional energy-process optimization).
- 3rd case: multidimensional optimization of the WaC/GaC length ratio and the shell side temperature with the objective of maximizing the methanol mole fraction (Multidimensional process optimization).
- 4th case: another multidimensional optimization of the WaC/GaC length ratio and the shell side temperature was made; this time the objective function has the objective to maximize the methanol mole fraction and the steam generation as well (so called multidimensional energy-process optimization).

An additional multidimensional optimization of the WaC/GaC length ratio, shell temperature and feed's temperature was performed to maximize methanol fraction and steam production, nonetheless, as observed in the sensitivity analysis, the system is not significantly affected by the modification of the feed's temperature and for instance, the results does not imply a greater improvement over the fourth step.

5.3.1 First case (Monodimensional process optimization)

In this particular case, the target is the maximization of the methanol yield throughout a single degree of freedom. The interesting parameter to optimize is the WaC/GaC reactor length ratio, which is roughly assumed equal to 0.7/0.3 for the industrial best practice in many cases. The optimization problem is formulated in Equation 5.6.

$$\max_{WaC/GaC\ length\ ratio} \quad y_{MeOH} \qquad 5.6$$

$$\text{s. t: WaC and GaC models (DAE)}$$

A penalty function was used in order to avoid achieving temperatures in the tube side where the catalyst will suffer deactivation by sintering (see Equation 5.7); this temperature was fixed to a value 0f 540 K in accordance with Løvik, Hillestad & Hertzberg, 1998 [33].

$$PF = \omega \cdot (T_{tube} - 540) \qquad 5.7$$

Where ω is a proper weight value. An economic objective function was proposed in order to maximize methanol yield, revenue from methanol was calculated in a yearly basis and the price[1] of methanol was taken as 370 €/t according to Methanex published prices [37]

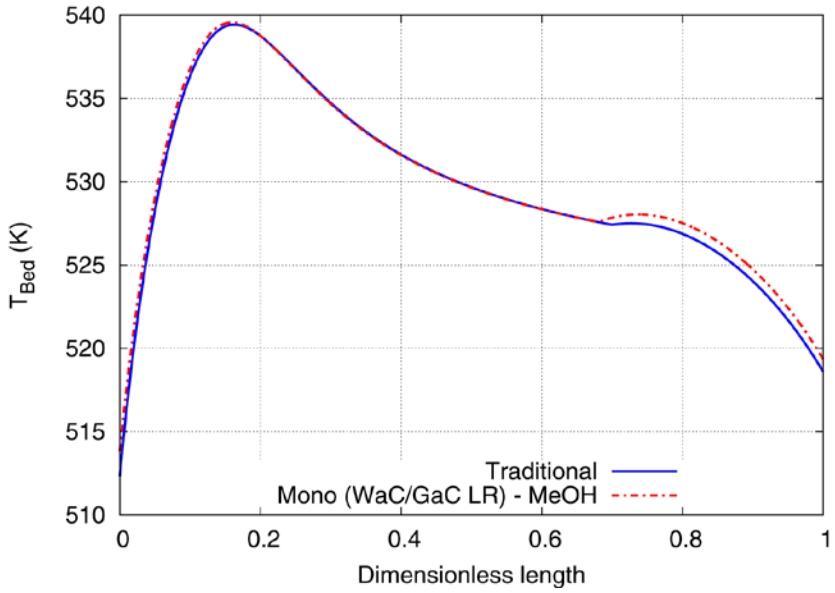

Figure 5-2 Comparison of the tube side temperature profile between the traditional configuration and the first case optimization.

[1] European price for the January 1 to March 31 period.

A comparison of tube side temperature profile and methanol mole fraction profile between the traditional configuration and the first optimization are reported in Figure 5-2 and Figure 5-3. As can be seen, both profiles are similar, suggesting that the traditional configuration is based on an already optimized system, as expected.

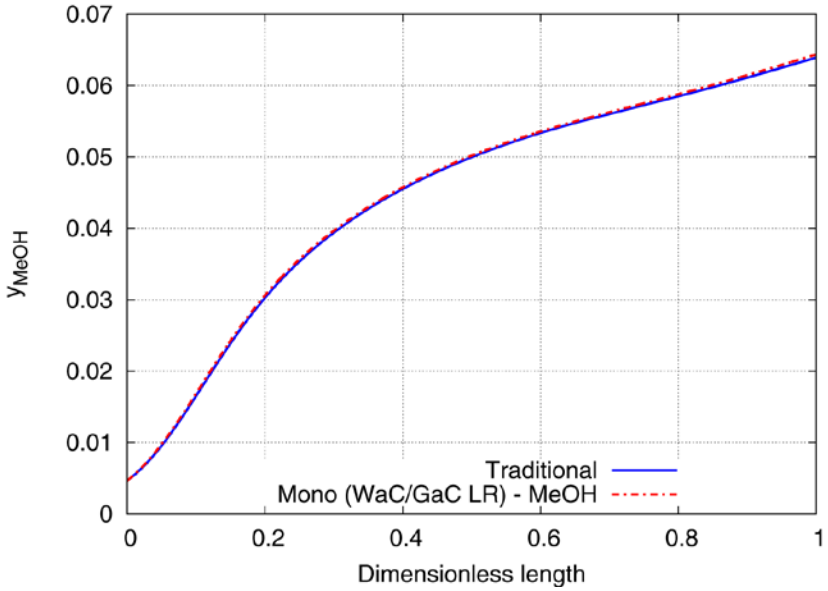

Figure 5-3 Comparison of methanol mole fraction profile between the traditional configuration and the first case optimization.

As CO and CO_2 are in opposite sides of the water gas shift reaction, a carbon conversion fraction was define (see Equation 5.8) to avoid interference of CO or CO_2 being consumed or produced, therefore the assessment of methanol synthesis is independent of the extent of the WGS reaction.

$$Carbon\ Conversion = \frac{\left(F_{CO} + F_{CO_2}\right)_{inlet} - \left(F_{CO} + F_{CO_2}\right)_{outlet}}{\left(F_{CO} + F_{CO_2}\right)_{inlet}} \qquad 5.8$$

In Table 5-1 are compared the values of the carbon conversion, methanol mole fraction and detailed revenue for both traditional and first case optimization.

Table 5-1 Comparison between results of traditional configuration and first case optimization.

		Traditional	First Case
Length ratio	-	0.7/0.3	0.68/0.32
Carbon conversion	-	0.2149	0.2212
Methanol mole fraction	-	0.063922	0.064357
Steam produced	GJ/y	190,295	191,116
Revenue from steam	€/y	5,285,997	5,308,781
Total revenue	€/y	45,844,440	46,067,784

It can be seen that, in accordance to the results shown before, difference between both cases is not significant as only an additional 0.68% in methanol yield was obtained and similarly, an improvement of only 0.49% in total revenue is achieved in the first case optimization.

5.3.2 Second case optimization (Monodimensional energy-process optimization)

The second case is intended to the maximization of methanol yield and steam generation; once again, with a single degree of freedom that is the WaC/GaC length ratio as formulated in Equation 5.9.

$$\max_{WaC/GaC\ length\ ratio} \quad y_{MeOH} + F_{Steam} \qquad 5.9$$
$$\text{s. t: WaC and GaC models (DAE)}$$

Similar to the first case, a penalty function was used as described in Equation 5.7 and an economic objective function was employed to the maximization of both methanol yield and steam generation, the latter was also assessed using an economical approach in which the price of energy was fixed as 0.1 €/kJ[2].

[2] Internal communication

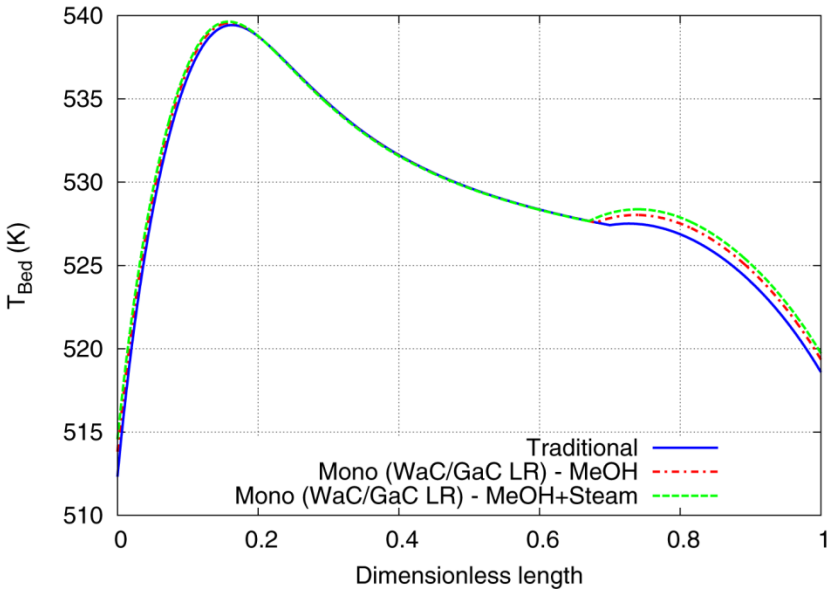

Figure 5-4 Comparison of the tube side temperature profile between the traditional configuration, the first case and the second case optimization.

As seen in Figure 5-4, the introduction of the steam generation did not modify any further the results obtained in the first case optimization, the same result can be appreciated in Figure 5-5 where there is no significant improvement in methanol yield.

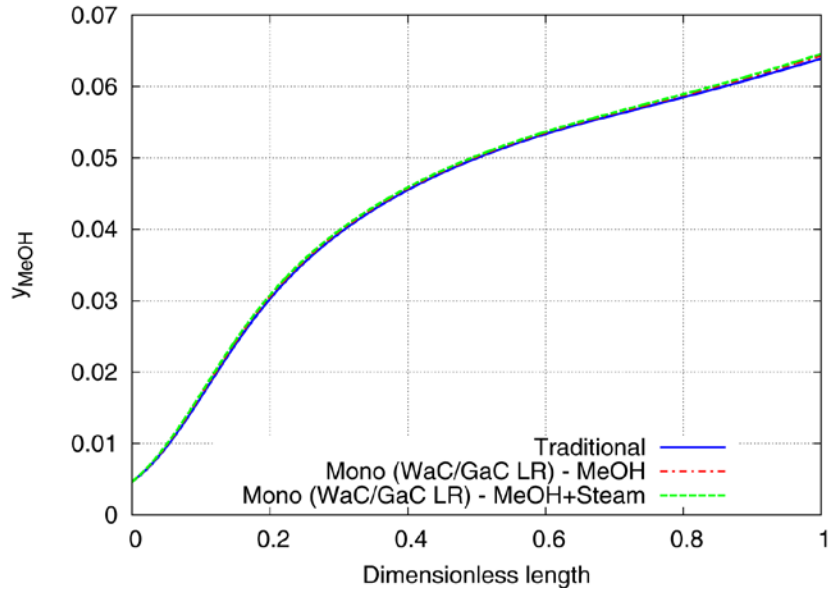

Figure 5-5 Comparison of methanol mole fraction profile between the traditional configuration, the first case and the second case.

According to the results obtained in Table 5-2, difference between the second case and the traditional configuration is about 1.02%, 0.62% and 0.72% in methanol yield, steam generation revenue and total revenue respectively.

Table 5-2 Comparison between results of traditional configuration, first case and second case optimization.

		Traditional	First Case	Second Case
Length ratio	-	0.7/0.3	0.68/0.32	0.67/0.33
Carbon conversion	-	0.2149	0.2212	0.2238
Methanol mole fraction	-	0.063922	0.064357	0.064575
Steam produced	GJ/y	190,295	191,116	191,483
Revenue from steam	€/y	5,285,997	5,308,781	5,318,972
Total revenue	€/y	45,844,440	46,067,784	46,178,091

The results obtained here and in section 5.3.1 shows that the optimization of a single degree of freedom did not introduce any advantage in the staged design of the methanol synthesis network suggesting that the traditional configuration is already optimized this way; however this approach does not allow any flexibility on the design, this is introduced by the utilization of further degrees of freedom which results in a higher complexity but allows to generate synergy between variables that could introduce further benefits to the final design.

5.3.3 Third case (Multidimensional process optimization)

The third case was dedicated to the optimization of the WaC/GaC length ratio and the shell side temperature with the scope of maximizing the methanol mole fraction as seen in Equation 5.10.

$$\max_{\substack{WaC/GaC\ ratio \\ WaC\ shell\ temp}} \quad y_{MeOH} \qquad 5.10$$

s. t: WaC and GaC models (DAE)

Figure 5-6 shows the comparison of tube side temperature for the traditional configuration and the fourth case, it can be observed that the introduction of an additional degree of freedom allows to modify extensively the staged design of the reactor allowing the improvement of the objective function, as a result, a second hot spot is developed suggesting that the kinetics of reaction is still active in the last stage of the reactor.

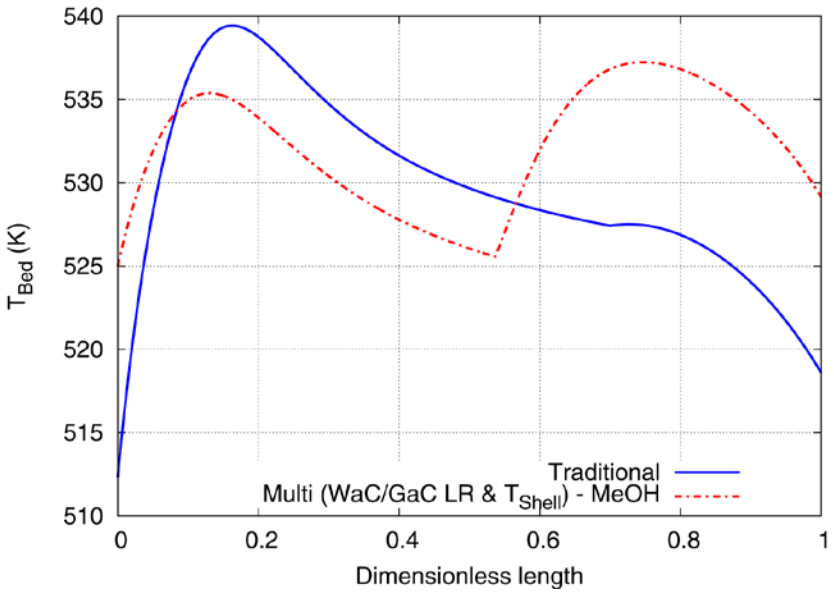

Figure 5-6 Comparison of the tube side temperature profile between the traditional configuration and the third case optimization.

The presence of a second hot spot is beneficial as it allows increasing the yield of methanol as can be observed in Figure 5-7 overcoming, to some extent, the unfavorable equilibrium thermodynamics of methanol synthesis reaction. On the other hand an improvement in steam generation was also obtained even when it is out of the scope of the maximization problem.

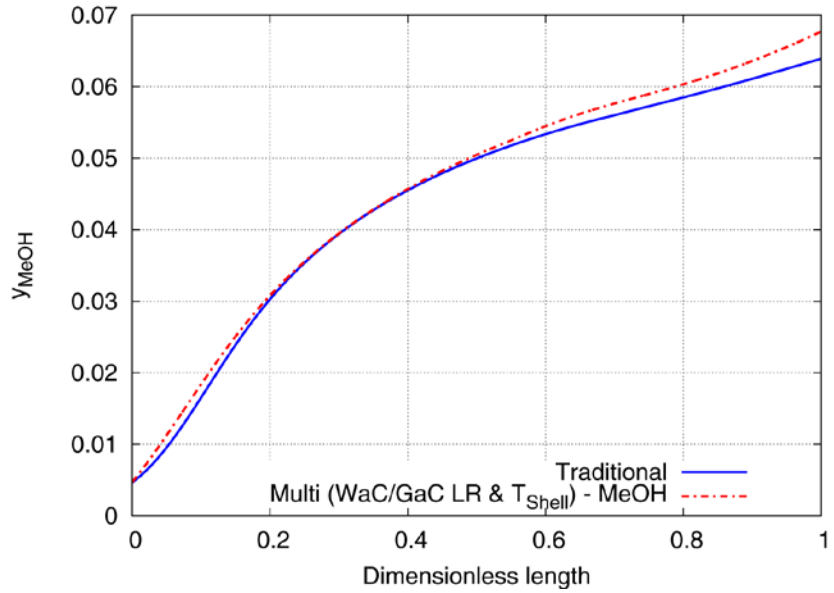

Figure 5-7 Comparison of methanol mole fraction profile between the traditional configuration and the third case optimization.

As a result a relevant improvement of 5.92% and 3.68% in methanol yield and total revenue are obtained respectively as seen in Table 5-3; this leads to about 1.7 M€ of additional profit per year in a medium size methanol plant.

Table 5-3 Comparison between results of traditional configuration and third case optimization.

		Traditional	Third Case
Length ratio	-	0.7/0.3	0.54/0.46
Shell side temperature	K	524	520.09
Carbon conversion	-	0.2149	0.2914
Methanol mole fraction	-	0.063922	0.067703
Steam produced	GJ/y	190,295	193,683
Revenue from steam	€/y	5,285,997	5,380,101
Total revenue	€/y	45,844,440	47,529,778

5.3.4 Fourth case (Energy-Process optimization)

The objective of the fourth case is the maximization of both methanol yield and steam generation, similar to the third case; two degrees of freedom were employed as described in Equation 5.11.

$$\max_{\substack{WaC/GaC\ ratio \\ WaC\ shell\ temp}} \quad y_{MeOH} + F_{Steam} \qquad 5.11$$

s. t: WaC and GaC models (DAE)

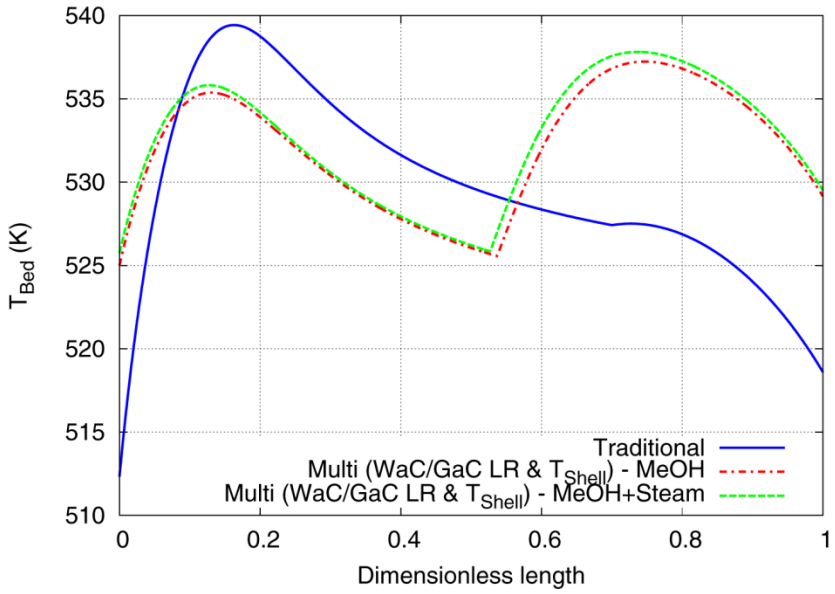

Figure 5-8 Comparison of the tube side temperature profile between the traditional configuration, the third case and the fourth case optimization.

From Figure 5-8 it's possible to appreciate that the results obtained here are similar to those in section 5.3.3, which is more evident for the methanol mole fraction in Figure 5-9.

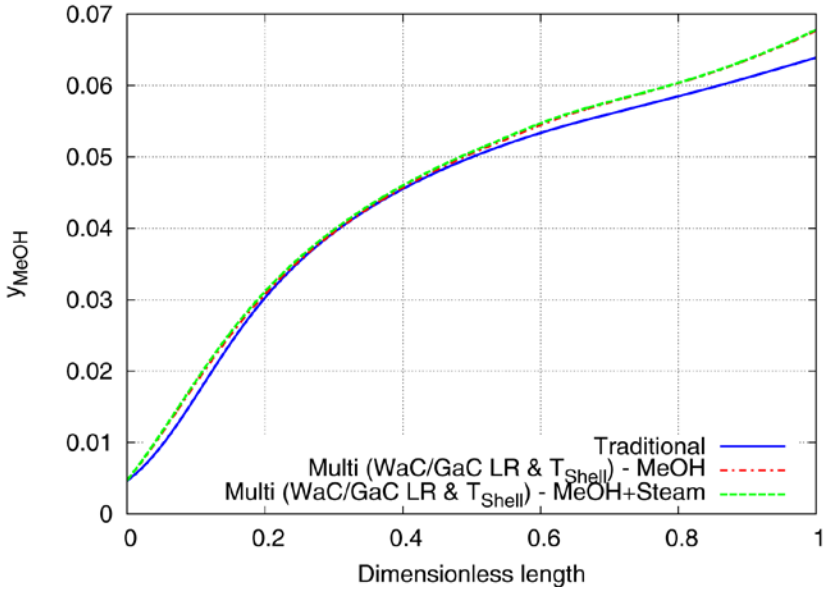

Figure 5-9 Comparison of methanol mole fraction profile between the traditional configuration, the third case and the fourth case.

This suggest that the optimization leads to the maximization of methanol yield as such variable is more significant in economic terms than the steam generation. Nonetheless, steam generation was also maximized but in a lesser extent.

Table 5-4 Comparison between results of traditional configuration, third case and fourth case optimization.

		Traditional	Third Case	Fourth Case
Length ratio	-	0.7/0.3	0.54/0.46	0.53/0.47
Shell side temperature	K	524	520.09	520.02
Carbon conversion	-	0.2149	0.2914	0.2977
Methanol mole fraction	-	0.063922	0.067703	0.06782
Steam produced	GJ/y	190,295	193,683	193,736
Revenue from steam	€/y	5,285,997	5,380,101	5,381,573
Total revenue	€/y	45,844,440	47,529,778	47,580,869

As seen in Table 5-4, an improvement of about 6.1%, 3.79% and 1.81% in methanol yield, total revenue and revenue from steam generation are obtained respectively.

The implementation of a systematic staging provides a flexible and comprehensive design of reactor networks if suitable and sufficient variables are employed as degrees of freedom in the optimization, even when the complexity of the design is further increased, the

benefits of a staged design surpasses such limitations as seen in the previous studied cases. Nonetheless, it is important to note that in order to achieve a more comprehensive result; a broad economic study should be made including the costs derived from a complex design, or even more to include this approach to plant-wide or enterprise wide optimizations.

5.4 Direct dimethyl ether synthesis process optimization

As already stated, literature works on the direct dimethyl ether synthesis is poor as it's still an ongoing research topic and most of the works available are based on the utilization of the WaC reactor almost exclusively, on the other hand, the data available from these works is uneven or the methodology adopted is not compatible with the formulation of the present thesis work. As a result a different approach was implemented for the optimization strategy.

- Base case: a monodimensional optimization of the inlet's molar feed flow of a WaC reactor with the objective of maximizing the methanol yield, the dimethyl ether yield and the carbon conversion.

This optimization procedure will provide a base case that will be further subject to systematic staging design as follows:

- 2nd case: a multidimensional optimization of the WaC/GaC length ration and the shell side temperature in order to maximize the methanol yield, the dimethyl ether yield and the steam generation.

As explained in section 5.3 the most benefit was obtained when using more than one degree of freedom as this provides greater flexibility on the design, as a result the monodimensional optimization was dropped in favor of a single multidimensional optimization.

5.4.1 First case (Inlet molar flow optimization)

As observed in Equation 5.12, this first case is intended for the optimization of the optimization of the inlet molar feed flow with the scope of optimizing the methanol and dimethyl ether yield; and the carbon conversion.

$$\max_{Inlet\ molar\ feed\ flow} \quad y_{MeOH} + y_{DME} + Carbon\ conversion \qquad 5.12$$

s. t: WaC model (ODE)

Once more, it is worth noting that a penalty function on the tube side temperature was implemented as seen in equation 5.7, this in order to avoid reaching temperatures above 540 K as it will result in permanent damage in the metallic function of the catalyst. To evaluate the yield of dimethyl ether and to afterwards optimize such parameter, an economic objective function was used; the price of dimethyl ether was taken from Fornell, Berntsson & Åsblad, [20] and is about 665 €/t.

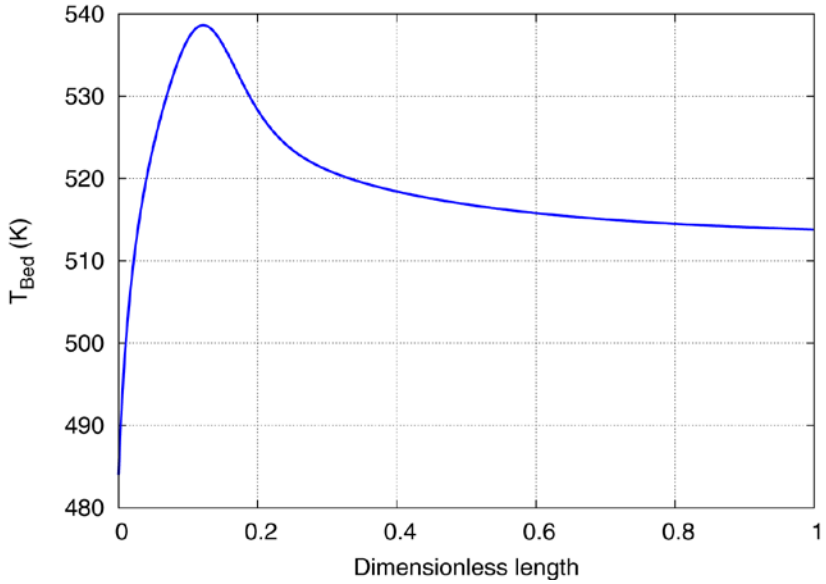

Figure 5-10 Tube side temperature profile for the base case.

From Figure 5-10 it can be seen that a single hot spot was developed as there is no GaC stage, as explained before, the sharper increase in the temperature profile in comparison with the methanol synthesis profile (see Figure 4-2) is caused by the superior exothermicity of the direct dimethyl ether synthesis reaction.

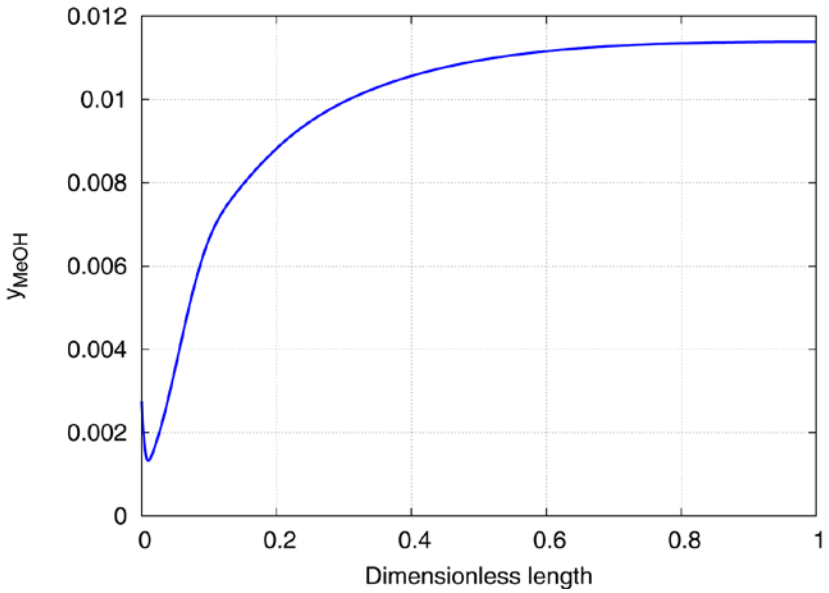

Figure 5-11 Methanol mole fraction profile for the base case.

Figure 5-11 shows that the inlet methanol fraction drops abruptly in the initial portion of the reactor, this suggest that the kinetics of dimethyl ether reaction is fast enough to star consuming methanol even in this first part of the reactor.

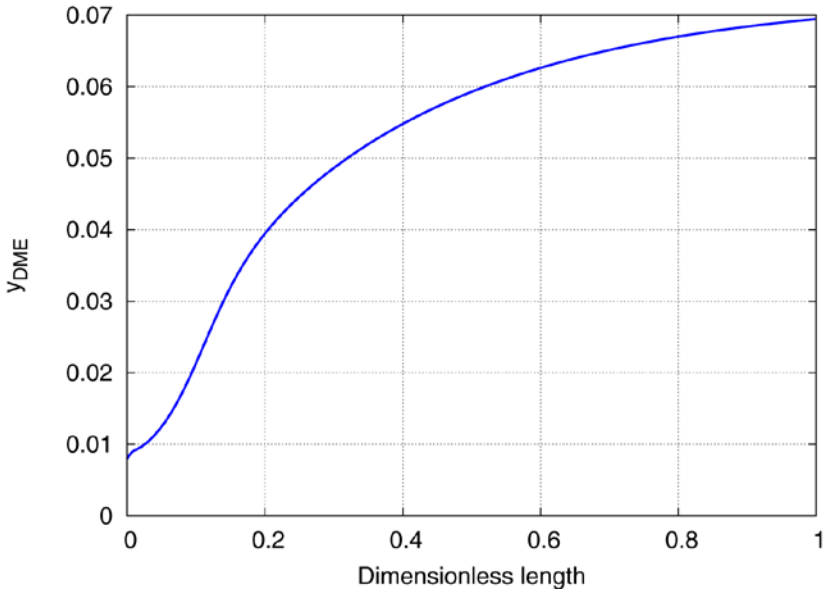

Figure 5-12 Dimethyl ether mole fraction profile for the first case.

It can be observed from Figure 5-11 and Figure 5-12 that the yield of both dimethyl ether and methanol is compressively higher than the yield of methanol in the methanol synthesis process. In fact, from Table 5-5 it is possible to see that the conversion of syngas is higher in comparison to the one obtained in the methanol synthesis process (see section 5.3)

which demonstrates the benefits of the synergic effect of coupling both systems of reactions.

Table 5-5 Data obtained from the base case of dimethyl ether synthesis.

		Base case
Length ratio	-	1.0/0.0
Carbon conversion	-	0.5038
Methanol mole fraction	-	0.011388
Revenue from methanol	€/y	1,729,037
Dimethyl ether mole fraction		0.069311
Revenue from dimethyl ether	€/y	27,222,006
Steam produced	GJ/y	207,021
Revenue from steam	€/y	5,750,589
Total revenue	€/y	34,701,633

5.4.2 Second case (Energy-process optimization)

Finally, an optimization of both WaC/GaC length ration and shell temperature was done to maximize methanol yield, dimethyl ether yield and steam generation as seen in Equation 5.13.

$$\max_{\substack{WaC/GaC\ ratio \\ WaC\ shell\ temp}} \quad y_{MeOH} + y_{DME} + F_{Steam} \qquad 5.13$$

s. t: WaC and GaC model (DAE)

It can be seen from Figure 5-13 that, as expected, the introduction of the GaC reactor rises the inlet tube side temperature of the WaC stage, nonetheless even when this enhances the kinetics of reaction, it does not provide any improvement in the final yield of dimethyl ether as seen in Figure 5-15, and only a subtle improvement is seen in methanol yield is obtained (see Figure 5-14) as tube side temperature drops in the final stage of the reaction improving the thermodynamic equilibrium of the reaction of the methanol synthesis reaction.

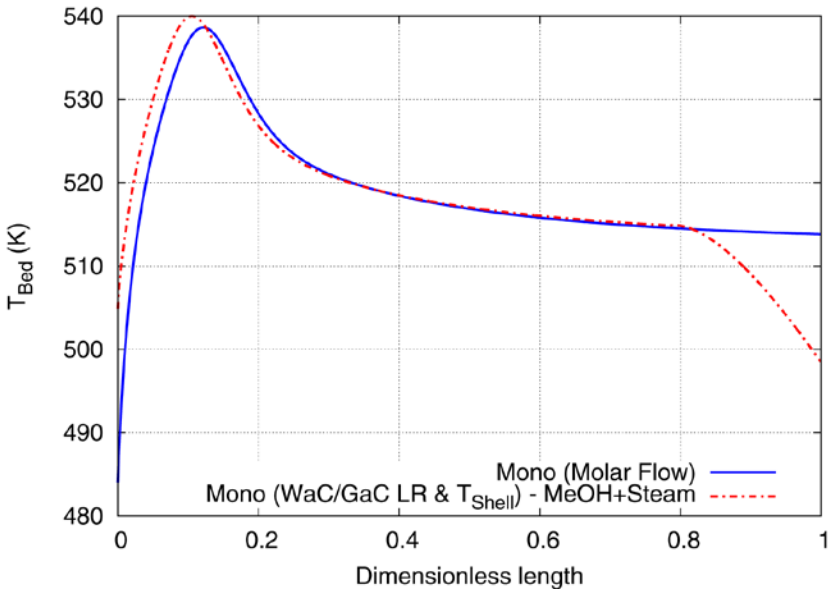

Figure 5-13 Tube side temperature profile comparison between the base case and the second case.

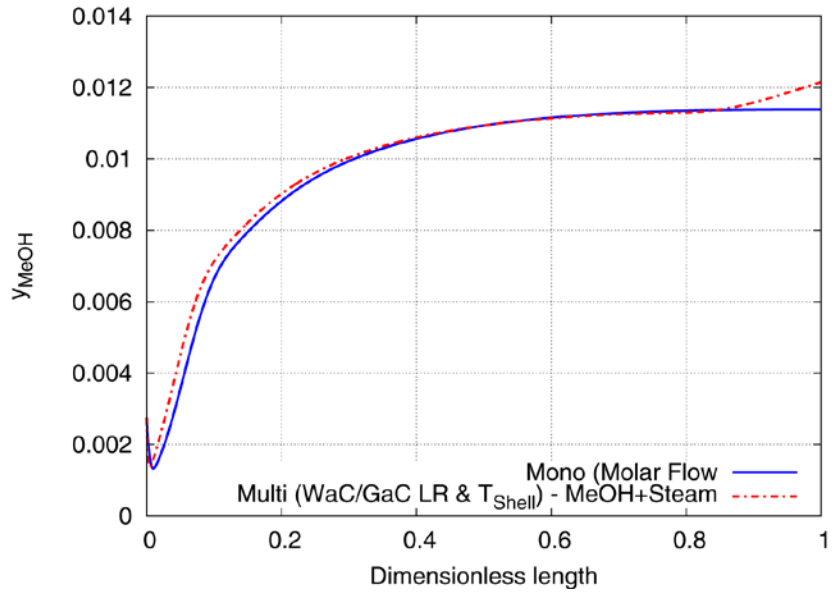

Figure 5-14 Methanol mole fraction profile comparison between the base case and the second case.

Many authors agree with that the dimethyl ether synthesis reaction is essentially kinetically controlled [28] and therefore the synergic effect of coupling both set of reactions makes the overall system kinetically controlled as well, as a result, in this particular case a systematic staging approach did not provide any improvement in the final design as the reaction kinetics is developed almost entirely in the first portion of the WaC reactor and therefore is not extended in the GaC reactor (like in methanol synthesis in section 5.3) so its introduction does not change substantially the final results.

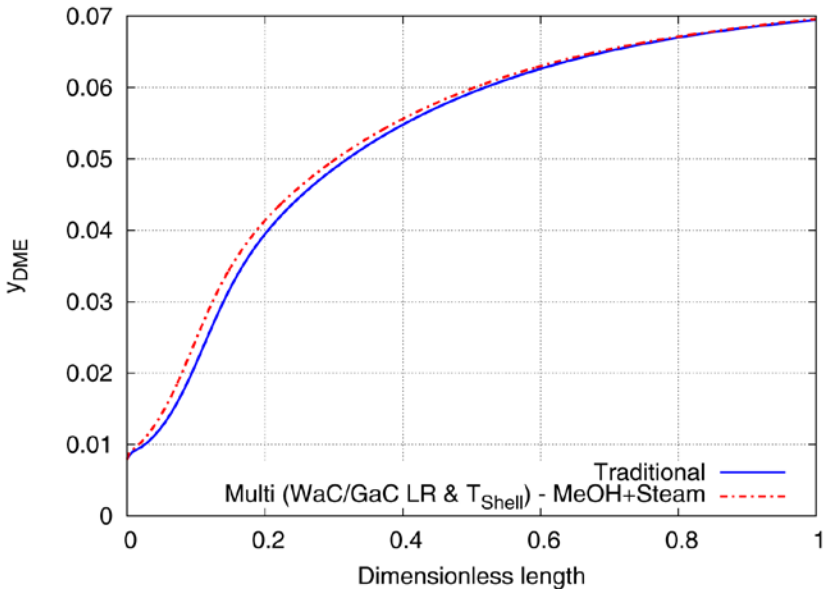

Figure 5-15 Dimethyl ether mole fraction profile comparison between the base case and the second case.

From Table 5-6 it is possible to see that, according to what has been mentioned above, the largest variation is in methanol yield (6.69%) as the reaction to produce this really takes advantage of the systematic staging approach. As for dimethyl ether yield, steam production and total revenue an improvement of 0.43%, 2.56% and 0.90% is obtained respectively.

Table 5-6 Data comparison between the base case and the second case in dimethyl ether optimization.

		Base case	Second case
Length ratio	-	1.0/0.0	0.78/0.22
Shell temperature	K	513	513.4
Carbon conversion	-	0.5038	0.5087
Methanol mole fraction	-	0.011388	0.012150
Revenue from methanol	€/y	1,729,037	1,840,402
Dimethyl ether mole fraction		0.069311	0.069612
Revenue from dimethyl ether	€/y	27,222,006	27,276,831
Steam produced	GJ/y	207,021	212,312
Revenue from steam	€/y	5,750,589	5,897,576
Total revenue	€/y	34,701,633	35,014,810

It is important to notice that the staged design is inclined towards obtaining a higher yield of dimethyl ether as the objective function is more sensitive to this parameter thanks to the higher price of DME in comparison with methanol and steam. In consequence, the systematic staging approach employed here could be implemented in a market driven

optimization methodology that takes account the possible fluctuation in the market; this will provide a tool for developing more flexible and comprehensive designs.

Conclusions

In this work, a techno economical assessment of the methanol synthesis process and the direct dimethyl ether synthesis process is addressed throughout a systematic staging methodology.

A reactor network composed of the water-cooled and the gas-cooled fixed-bed reactors of the Lurgi-type process and a separation and recycle system were modeled. Usually the gas-cooled reactor is neglected in literature works, nonetheless in order to provide a comprehensive economical assessment it was included as well in this thesis project.

The resulting phenomenological mathematical is composed by a set of ordinary differential equations coupled with algebraic constraints and a combination of initial and boundary conditions so its solution has been possible with the employment of the *BzzMath* library. Subsequently, the systematic staging approach was achieved by means of an economical multidimensional non-linear optimization of the reactor network also with the aid of the *BzzMath* library.

The results showed that considering the GaC stage of the reactor is not only important to make a complete techno-economical assessment but also provides benefits in overcoming the drawbacks of the thermodynamic equilibrium in the methanol synthesis reaction. As a result a revision on the design could increase by about 1.7 M€/y the net operating margin of a medium size methanol plant.

As the direct dimethyl ether synthesis, the introduction of a systematic staging GaC stage did not bring any improvement over the final design; nonetheless the real benefit comes from coupling the reaction system involved in methanol synthesis to the reaction system of dimethyl ether synthesis thanks to the synergic effect that alleviates the methanol

synthesis equilibrium limitation, therefore increasing the carbon conversion that is expected to minimize the compression costs in the recycle.

As the systematic staging approach provides further flexibility on the design by the integration of multiple degrees of freedom resulting in an improvement of the objective function, it could provide a valuable tool if such approach is extended into plant-wide optimization or even an enterprise-wide optimization where process adaptability is needed. Thus, it could pave the way for a 'market driven' process optimization.

On the other hand, the model is adapted to the study of the effect of utilization of syngas originated from non-traditional feedstocks such as biomass or biogas, to keep in line with present research topics.

Appendix A

Kinetics and thermodynamics of methanol synthesis reaction

Kinetic parameters

The kinetic parameters and the adsorption equilibrium constants were obtained from Graaf, Scholtens, Stamhuis & Beenackers, 1990 [21]:

$$
\begin{aligned}
k_1 &= 4.89 \times 10^7 \cdot e^{-\frac{113000}{RT}} \\
k_2 &= 9.641 \times 10^{11} \cdot e^{-\frac{152900}{RT}} \\
k_3 &= 1.09 \times 10^5 \cdot e^{-\frac{87500}{RT}} \\
K_{CO} &= 2.16 \times 10^{-5} \cdot e^{\frac{98388}{RT}} \\
K_{CO_2} &= 7.05 \times 10^{-7} \cdot e^{\frac{61700}{RT}} \\
K_{H_2O}/K_{H_2}^{0.5} &= 6.37 \times 10^{-9} \cdot e^{\frac{84000}{RT}}
\end{aligned}
\qquad \text{A.1}
$$

Where R is the gas constant in J/mol/K ,T is the temperature in K, K_i is the adsorption constant in in Pa and k_i is in mol/kg_{cat}/s.

Thermodynamic parameters

The chemical equilibrium constants were obtained from Graaf & Beenackers, 1996 [23].

$$
\begin{aligned}
K_{p1} &= 2.391 \times 10^{-13} \cdot e^{\frac{98388}{RT}} \\
K_{p2} &= 1.068 \times 10^{2} \cdot e^{-\frac{39683}{RT}} \\
K_{p3} &= 2.554 \times 10^{-11} \cdot e^{\frac{58705}{RT}}
\end{aligned}
\qquad \text{A.2}
$$

Where R is the gas constant in J/mol/K and T is the temperature in K

Reactor specifications

In Table A-1 are listed the reactor specifications employed in the present thesis work.

Table A-1 Methanol synthesis reactor specifications

Total length	7	m
D_i	0.0341	m
D_o	0.0381	m
Bed density	1770	kg/m^3
Particle's diameter	5.47×10^{-3}	m
Void fraction	0.39	-
Number of tubes	2962	-

These specifications were assumed from the papers of Rahimpour, 2008 [44] and Abrol & Hilton,2012 [1].

Correlations for the estimation of physical properties

Vapor viscosity estimation

Viscosities of pure substances in vapor phase were calculated using the correlations reported on Green and Perry, 2007 [24]. Vapor viscosity of the mixture was calculated using Wilke's method reported on Poling, Praustnitz & Connell, 2001 [42]:

$$\mu_m = \sum_{i=1}^{n} \frac{y_i \mu_i}{\sum_{j=1}^{n} y_i \phi_{ij}} \qquad \text{A.3}$$

$$\phi_{ij} = \frac{\left[1 + \left(\mu_i/\mu_j\right)^{1/2} \left(M_j/M_i\right)^{1/4}\right]^2}{\left[8\left(1 + M_i/M_j\right)\right]^{1/2}} \qquad \text{A.4}$$

Where μ_i and μ_j are the viscosities of the i-th and j-th component; M_i and M_j are the molar masses of the i-th and j-th component; and μ_m is the mixture's vapor viscosity.

Vapor thermal conductivity estimation

Thermal conductivities of pure substances in vapor phase were calculated using the correlations reported on Green and Perry, 2007 [24]. Thermal conductivity of the mixture was calculated using the Mason and Saxena method reported on Poling et al., 2001 [42]:

$$k_m = \sum_{i=1}^{n} \frac{y_i k_i}{\sum_{j=1}^{n} y_i A_{ij}} \qquad \text{A.5}$$

$$A_{ij} = \phi_{ij} = \frac{\left[1 + \left(\mu_i/\mu_j\right)^{1/2} \left(M_j/M_i\right)^{1/4}\right]^2}{\left[8\left(1 + M_i/M_j\right)\right]^{1/2}} \qquad \text{A.6}$$

Where k_i and k_j are the thermal conductivities of the i-th and j-th component; μ_i and μ_j are the viscosities of the i-th and j-th component; M_i and M_j are the molar masses of the i-th and j-th component; and k_m is the mixture's thermal conductivity.

Effective diffusivity estimation

Diffusivity of pure substances in vapor phase was calculated using the Fuller Schettler Giddings (FSG) correlation reported on Poling et al., 2001 [42]:

$$D_{AB} = \frac{0.00143 \cdot T^{1.75}}{P \cdot M_{AB}^{1/2} \cdot \left[(\sum v)_A^{1/3} + (\sum v)_B^{1/3}\right]} \qquad \text{A.7}$$

Where T is temperature in K, P is the pressure in bar and M_{AB} is given by:

$$M_{AB} = 2 \cdot \left[\left({}^{1}/_{M_A}\right) + \left({}^{1}/_{M_B}\right)\right]^{-1} \qquad \text{A.8}$$

M_A and M_B are the molar weights of the species A and B. $\sum v$ are the atomic diffusion volumes and are reported on Table A-2.

Table A-2 Atomic diffusion volumes of the species.

CO	18.9
CO_2	26.9
H_2	7.07
H_2O	12.7
CH_3OH	29.9
N_2	17.9
DME	51.77
CH_4	24.42

Diffusivity of a species in a mixture was using the Wilke method reported in Green and Perry, 2007 [24]:

$$D_{im} = \left(\sum_{\substack{j=1 \\ j \neq i}}^{N_C} \frac{x_j}{D_{ij}} \right)^{-1} \qquad \text{A.9}$$

Where x_j is the molar fraction of the j-th species. Finally the effective diffusivity of the gases through the porous catalyst is calculated with the expression reported in Green and Perry, 2007 [24]:

$$D_{i,eff} = D_{im} \frac{\epsilon_c}{\tau} \qquad \text{A.10}$$

Where ϵ_c and τ are the porosity and the tortuosity of the catalyst respectively.

Correlations for the prediction of heat transfer coefficients

Convective heat transfer coefficient for boiling systems

The Mostinski equation was used for the calculation of the boiling heat transfer coefficient as reported on Green & Perry, 2007 [24]:

$$h = 3.75 \times 10^{-5} P_c^{0.69} \left(\frac{q}{A}\right)^{0.7} \left[1.8 \left(\frac{P}{P_c}\right)^{0.17} + 4 \left(\frac{P}{P_c}\right)^{1.2} + 10 \left(\frac{P}{P_c}\right)^{10} \right] \qquad \text{A.11}$$

The maximum heat flux $^{q}/_{A}$ is calculated from the Cichelli-Bonilla correlation also reported on Green & Perry, 2007 [24]:

$$\frac{(^{q}/_{A})_{max}}{P_c} = 0.368\left(\frac{P}{P_c}\right)^{0.35}\left(1-\frac{P}{P_c}\right)^{0.9} \qquad \text{A.12}$$

For the above equations P is the system pressure and P_c is the critical pressure.

Convective heat transfer coefficient for flow around tube

The convective heat coefficient for the flow around the tube was calculated using the Churchill and Bernstein correlation reported on Green & Perry, 2007 [24]:

$$\overline{\mathrm{Nu}_D} = 0.3 + \frac{0.62\mathrm{Re}_D^{1/2}\mathrm{Pr}^{1/3}}{[1+(0.4/\mathrm{Pr})^{2/3}]^{1/4}}\left[1+\left(\frac{\mathrm{Re}_D}{282000}\right)^{5/8}\right]^{4/5} \qquad \text{A.13}$$

Where $\mathrm{Re_D}$ is the Reynolds number across the tube, Pr is the Prandtl number and Nu is the Nusselt number.

Convective heat transfer coefficient for flow through a fixed bed

For both WaC and GaC stages a Chilton and Colburn J-analogy was used as described by Smith, [47] 1983:

$$J_H = \frac{h}{C_P G}\left(\frac{C_P\mu}{k_f}\right) \qquad \text{A.14}$$

$$J_D = \frac{0.458}{\epsilon_B}\left(\frac{d_p G}{\mu}\right)^{-0.407} \qquad \text{A.15}$$

$$J_D = J_H \qquad \text{A.16}$$

Where C_P is the specific heat in J//mol/K), μ is the viscosity in Pa·s, d_p is the particle's diameter in m, ϵ_B is the void fraction, k_f is the fluid conductivity in W/m/K, G is the mass

velocity based on superficial area kg/s/m^2 and h is the convective heat coefficient in W//m^2/K.

Overall heat transfer coefficient

The overall heat transfer coefficient is calculated as:

$$U = \left[\frac{1}{h_i} + \frac{A_i \ln\left(\frac{D_o}{D_i}\right)}{2\pi L k} + \frac{A_i}{A_o h_o}\right] \qquad \text{A.17}$$

Where h_i and h_o are respectively the internal and external convective heat transfer coefficients, A_i and A_o are the respectively the internal and external heat transfer area, D_i and D_o are respectively the internal and external tube diameter, L is the length of the tube and k is thermal conductivity of the material employed for the tube.

Appendix B

Kinetics and thermodynamics of dimethyl ether synthesis reaction

Kinetic parameters

The kinetic parameters and were obtained from Song et al., 2008 [48] and the equilibrium constant from Diep & Wainwright, 1987 [14]:

$$k_4 = 1.028 \times 10^{10} \cdot e^{-\frac{105000}{RT}}$$
$$K_{CH_3OH} = 7.9 \times 10^{-7} \cdot e^{\frac{70500}{RT}} \qquad \text{A.18}$$
$$K_{H_2O} = 8.47 \times 10^{-5} \cdot e^{\frac{41100}{RT}}$$

Where R is the gas constant in J/mol/K, T is the temperature in K, K_i is the adsorption constant in m^3/mol and k_i is in $mol/kg_{cat}/s$.

Thermodynamic parameters

$$K_c = \frac{2835.2}{T} + 1.675 \cdot \ln T - 2.39 \times 10^{-4} - 0.21 \times 10^{-6} \cdot T^2 - 13.36 \qquad \text{A.19}$$

Where R is the gas constant in J/mol/K and T is the temperature in K

Reactor specifications

Table B-1 Direct dimethyl ether reactor specifications

Total length	7	m
D_i	0.046	m
D_o	0.05	m
Bed density	1783.5	kg/m^3
Void fraction	0.39	-
Number of tubes	2962	-

The specification listed above are based in the works by Vakili & Eslamlouyean, 2012 [53], Song et al., 2008 [48] and Rahimpour, 2008 [44].

Correlations for the estimation of physical properties

The correlations employed to the prediction of physical properties are the same reported in Appendix A.

Correlations for the prediction of heat transfer coefficients

Regarding correlations for the prediction of heat transfer coefficients, the only difference between the methanol synthesis and the direct dimethyl ether synthesis is the utilization of the Rase correlation in the WaC reactor as reported on Yang, 2003 [57] to calculate the heat transfer coefficient for flow across a cylindrical vessel with spherical packing:

$$\overline{\mathrm{Nu}_D} = 2.26(\mathrm{Re}_P)^{0.8}\mathrm{Pr}^{0.33}\, e^{\left(-\frac{6d_P}{D}\right)} \qquad \text{A.20}$$

Where $\mathrm{Re_P}$ is the particle's Reynolds number, Pr is the Prandtl number, $\mathrm{Nu_D}$ is the Nusselt number, d_P is the particle's diameter and D the tube's diameter.

The GaC stage employed the J-analogy described in Appendix A.

References

[1] Abrol S, Hilton CM. Modeling, simulation and advanced control of methanol production from variable synthesis gas feed. Comput.Chem.Eng. 2012 MAY 11;40:117-31.

[2] Alamolhoda S, Kazemeini M, Zaherian A, Zakerinasab MR. Reaction kinetics determination and neural networks modeling of methanol dehydration over nano gamma-Al2O3 catalyst. J.Ind.Eng.Chem. 2012 NOV 25;18(6):2059-68.

[3] Arcoumanis C, Bae C, Crookes R, Kinoshita E. The potential of di-methyl ether (DME) as an alternative fuel for compression-ignition engines: A review. Fuel 2008 6;87(7):1014-30.

[4] Askari F, Rahimpour M, Jahanmiri A, Mostafazadeh A, Khosravanipour Mostafazadeh A. Dynamic Simulation and Optimization of a Dual-Type Methanol Reactor Using Genetic Algorithms. Chemical engineering technology 2008;31(4):513-24.

[5] Behrens M, Studt F, Kasatkin I, Kühl S, Hävecker M, Abild-Pedersen F, et al. The Active Site of Methanol Synthesis over Cu/ZnO/Al2O3 Industrial Catalysts. Science 2012 May 18;336(6083):893-7.

[6] Bercic G, Levec J. Intrinsic and global reaction rate of methanol dehydration over .gamma.-alumina pellets. Ind Eng Chem Res 1992 04/01; 2013/06;31(4):1035-40.

[7] Buzzi-Ferraris G. BzzMath: numerical library in C++. 2012; Available at: <http://chem.polimi.it/homes/gbuzzi>.

[8] Buzzi-Ferraris G. Ottimizzazione difunzioni a più variabili. Nota I.Variabili non vincolate. 1967;3:101.

[9] Buzzi-Ferraris G, Manenti F. Nonlinear Systems and Optimization for the Chemical Engineer Solving Numerical Problems. : John Wiley & Sons; 2013.

[10] Casale Group. Methanol Casale and Foster Wheeler: A New Alliance for the Methanol Industry. 2013; Available at: <http://casale.ch>.

[11] Chauvel A, Lefebvre G. Petrochemical processes. 1. Synthesis-gas derivatives and major hydrocarbons. : Gulf Publishing Company; 1989.

[12] S. Cieri, M. Restelli. Controllo ottimale basato su modelli di equazioni differenziale alle derivate parziali. Applicazione al reattore di sintesi del metanolo. Milan: Politecnico di Milano; 2009.

[13] Davy Process Technology Ltd. Methanol Technology. 2013; Available at: <http://www.davyprotech.com>.

[14] Diep BT, Wainwright MS. Thermodynamic equilibrium constants for the methanol-dimethyl ether-water system. J.Chem.Eng.Data 1987 07/01; 2013/06;32(3):330-3.

[15] E. DPS, J.A.J.M. Catalysis. : Royal Society of Chemistry; 2011.

[16] Erena J, Garona R, Arandes J, Aguayo A, Bilbao J. Effect of operating conditions on the synthesis of dimethyl ether over a CuO-ZnO-Al2O3/NaHZSM-5 bifunctional catalyst. Catal.Today 2005 OCT 30;107-08:467-73.

[17] Erena J, Sierra I, Aguayo AT, Ateka A, Olazar M, Bilbao J. Kinetic modelling of dimethyl ether synthesis from (H-2 + CO2) by considering catalyst deactivation. Chem.Eng.J. 2011 NOV 1;174(2-3):660-7.

[18] Fiedler E, Grossmann G, Kersebohm DB, Weiss G, Witte C. Methanol. Ullmann's Encyclopedia of Industrial Chemistry: Wiley-VCH Verlag GmbH & Co. KGaA; 2000.

[19] Fleisch TH, Basu A, Sills RA. Introduction and advancement of a new clean global fuel: The status of DME developments in China and beyond. Journal of Natural Gas Science and Engineering 2012;9:94-107.

[20] Fornell R, Berntsson T, Asblad A. Techno-economic analysis of a kraft pulp-mill-based biorefinery producing both ethanol and dimethyl ether. Energy 2013 FEB 1;50:83-92.

[21] Graaf GH, Scholtens H, Stamhuis EJ, Beenackers AACM. Intra-particle diffusion limitations in low-pressure methanol synthesis. Chemical Engineering Science 1990;45(4):773-83.

[22] Graaf GH, Stamhuis EJ, Beenackers AACM. Kinetics of low-pressure methanol synthesis. Chemical Engineering Science 1988;43(12):3185-95.

[23] Graaf G, Beenackers A. Comparison of two-phase and three-phase methanol synthesis processes. Chem.Eng.Process 1996;35(6):413-27.

[24] Green D, Perry R. Perry's Chemical Engineers' Handbook, Eighth Edition. : McGraw-Hill Education; 2007.

[25] Haldor Topsøe A/S. Topsøe Methanol Technology. 2013; Available at: <http://www.topsoe.com/>.

[26] Hillestad M. Systematic staging in chemical reactor design. Chem.Eng.Sci. 2010 MAY 15;65(10):3301-12.

[27] International Dimethyl Ether Association. IDA Fact Sheet No. 1 - DME/LPG Blends. 2010; Available at: <http://www.aboutdme.org>.

[28] Jia G, Tan Y, Han Y. A comparative study on the thermodynamics of dimethyl ether synthesis from CO hydrogenation and CO2 hydrogenation. Ind Eng Chem Res 2006 FEB 1;45(3):1152-9.

[29] Khandan N, Kazemeini M, Aghaziarati M. Direct production of dimethyl ether from synthesis gas utilizing bifunctional catalysts. Applied Petrochemical Research 2012 03/01;1(1-4):21-7.

[30] Kumar M, Srivastava V. Simulation of a Fluidized-Bed Reactor for Dimethyl Ether Synthesis. Chemical engineering technology 2010;33(12):1967-78.

[31] Lee S, Speight JG, Loyalka SK. Handbook of Alternative Fuel Technologies. : Taylor & Francis; 2007.

[32] Lommerts B, Graaf G, Beenackers A. Mathematical modeling of internal mass transport limitations in methanol synthesis. Chem.Eng.Sci. 2000 DEC;55(23):5589-98.

[33] Løvik I, Hillestad M, Hertzberg T. Long term dynamic optimization of a catalytic reactor system. Comput.Chem.Eng. 1998 3/15;22, Supplement 1(0):S707-10.

[34] Lurgi GmbH. Lurgi MegaMethanol®. 2013; Available at: <http://www.lurgi.com>.

[35] Manenti F, Cieri S, Restelli M. Considerations on the steady-state modeling of methanol synthesis fixed-bed reactor. Chemical Engineering Science 2011 1/15;66(2):152-62.

[36] McBride K, Turek T, Guettel R. Direct dimethyl ether synthesis by spatial patterned catalyst arrangement: A modeling and simulation study. AIChE J. 2012 NOV;58(11):3468-73.

[37] Methanex Corporation. Methanex Regional Posted Contract Prices. 2013; Available at: <http://www.methanex.com>.

[38] Moradi GR, Ahmadpour J, Yaripour F, Wang J. Equilibrium Calculations for Direct Synthesis of Dimethyl Ether from Syngas. Can.J.Chem.Eng. 2011 FEB;89(1):108-15.

[39] Murray J, King D. Climate policy: Oil's tipping point has passed. Nature 2012 01/26;481(7382):433-5.

[40] Nelder JA, Mead R. A simplex method for function minimization. The computer journal 1965;7(4):308-13.

[41] Olah G. Beyond oil and gas: the methanol economy. Angewandte Chemie (International ed.) 2005;44(18):2636-9.

[42] Poling BE, Prausnitz JM, O'Connell JP. The properties of gases and liquids. : McGraw-Hill Professional Publishing; 2001.

[43] Rachford Jr. HH, Rice JD. Procedure for Use of Electronic Digital Computers in Calculating Flash Vaporization Hydrocarbon Equilibrium. J.Pet.Technol. 1952;4(10).

[44] Rahimpour MR. A two-stage catalyst bed concept for conversion of carbon dioxide into methanol. Fuel Process Technol 2008;89(5):556-66.

[45] Seider WD, Seader JD, Lewin DR. Product and Process Design Principles: Synthesis, Analysis and Design, 3E with CD-ROM International Student Version. : John Wiley; 2010.

[46] Sierra I, ErenÌƒa J, Aguayo AT, Olazar M, Bilbao J. Deactivation Kinetics for Direct Dimethyl Ether Synthesis on a CuOâˆ'ZnOâˆ'Al2O3/Î³-Al2O3 Catalyst. Ind Eng Chem Res 2010 01/20; 2013/06;49(2):481-9.

[47] Smith JM. Chemical Engineering Kinetics. : McGraw-Hill; 1983.

[48] Song D, Cho W, Lee G, Park DK, Yoon ES. Numerical Analysis of a Pilot-Scale Fixed-Bed Reactor for Dimethyl Ether (DME) Synthesis. Ind Eng Chem Res 2008 07/01; 2013/06;47(13):4553-9.

[49] Spendley W, Hext GR, Himsworth FR. Sequential Application of Simplex Designs in Optimisation and Evolutionary Operation. Technometrics 1962 Nov.;4(4):441-61.

[50] Sun JT, Metcalfe IS, Sahibzada M. Deactivation of Cu/ZnO/Al2O3 Methanol Synthesis Catalyst by Sintering. Ind Eng Chem Res 1999 10/01; 2013/05;38(10):3868-72.

[51] Towler G, Sinnott RK. Chemical Engineering Design: Principles, Practice and Economics of Plant and Process Design. : Elsevier Science; 2007.

[52] U.S. Department of Energy. Commercial-Scale Demostration of the Liquid Phase Methanol (LPMEOH™) Process. 2013; Available at: <http://www.netl.doe.gov/>.

[53] Vakili R, Eslamloueyan R. Optimal design of an industrial scale dual-type reactor for direct dimethyl ether (DME) production from syngas. Chem.Eng.Process 2012 DEC;62:78-88.

[54] Wang Z, Wang J, Ren F, Han M, Jin Y. Thermodynamics of the single-step synthesis of dimethyl ether from syngas. Tsinghua Science and Technology 2004;9(2):168-76.

[55] Wender I. Reactions of synthesis gas. Fuel Process Technol 1996 9;48(3):189-297.

[56] Wood DA, Nwaoha C, Towler BF. Gas-to-liquids (GTL): A review of an industry offering several routes for monetizing natural gas. J.Nat.Gas Sci.Eng. 2012 NOV;9:196-208.

[57] Yang WC. Handbook of Fluidization and Fluid-Particle Systems. : Taylor & Francis; 2003.